

USRA

High Speed Civil Transport

N93-18161

Unclass

G3/05 0141642

(NASA-CR-192041) HIGH SPEED CIVIL
TRANSPORT (California State
Polytechnic Univ.) 108 p



Apogee Aeronautics Corporation

California State Polytechnic University, Pomona
Aerospace Engineering Department

TABLE OF CONTENTS

	Page
LIST OF FIGURES.....	iii
LIST OF TABLES.....	v
LIST OF SYMBOLS.....	vi
APOGEE AERONAUTICS CORPORATION.....	vii
EXECUTIVE SUMMARY.....	ix
1.0 INTRODUCTION	
1.1 Opportunity.....	1
1.2 Request For Proposal (RFP).....	2
1.3 Flight Profile.....	8
2.0 VEHICLE DEVELOPMENT	
2.1 Vehicle Concepts.....	10
2.2 Initial Configurations.....	18
2.3 Constraint Diagram.....	23
3.0 AERODYNAMICS	
3.1 Wing Design.....	24
3.2 High Lift Devices.....	26
3.3 Vertical Tail Design.....	28
3.4 Fuselage Design.....	30
4.0 PROPULSION SYSTEMS	
4.1 Engine Candidates.....	34
4.2 Engine Inlet System.....	36
5.0 STRUCTURAL ANALYSIS	
5.1 Structures (General).....	40
5.2 Material Selection.....	40
5.3 Thermal Management.....	43
5.4 Wing Structure.....	45
5.5 Fuselage Structure.....	49
5.6 Tail Structure.....	52
5.7 Landing Gear.....	52

6.0	PERFORMANCE	
6.1	Takeoff Distance.....	54
6.2	Range And Endurance.....	54
6.3	Landing Performance.....	58
6.4	Takeoff And Landing Visibility.....	59
6.5	Rate Of Climb.....	59
6.6	Rate Of Descent.....	60
7.0	STABILITY AND CONTROL ANALYSIS	
7.1	Subsonic.....	61
7.2	Cruise.....	63
7.3	Transonic.....	64
8.0	FUSELAGE INTERIOR LAYOUT	
8.1	Passenger Seating Arrangements.....	66
8.2	Capacity and Payload Accommodations.....	68
8.3	Interior Facilities.....	69
8.4	Doors, Emergency Exits, And Windows.....	69
9.0	MARKETABILITY	
9.1	Potential Markets.....	73
9.2	Airport Compatibility.....	74
9.3	Cost Analysis.....	77
10.0	MAINTENANCE AND RELIABILITY (M & R)	
10.1	Engine M & R.....	82
10.2	Material M & R.....	83
11.0	ENVIRONMENTAL IMPACT	
11.1	Sonic Boom.....	84
11.2	Engine Emissions.....	84
11.3	Engine Noise.....	87
12.0	FUTURE DESIGN RECOMMENDATIONS.....	92
13.0	REFERENCES.....	94

LIST OF FIGURES

		Page
FIGURE i-1	Supercruiser HS - 8.....	x
FIGURE 1-1	Flight Profile (a) Routine Mission Profile.....	8
	(b) Alternative Airport Selection.	9
FIGURE 2-1	Cylindrical Fuselage Configurations: Tupolev TU-144 "Charger".....	11
FIGURE 2-2	Proposed Large-Payload, Twin-Fuselage SST.....	12
FIGURE 2-3	Proposed Blended Wing-Body Arrangement Where Dimensions Are Given In Feet, Except As Noted...	13
FIGURE 2-4	Oblique Wing Configuration.....	14
FIGURE 2-5	Fixed Swept Wing Configuration.....	15
FIGURE 2-6	Variable Sweep Wing Configuration.....	15
FIGURE 2-7	Double Delta / Cranked Arrow Configurations: Tupolev TU-144 "Charger".....	16
FIGURE 2-8	Proposed Oblique Wing Configuration For A Future SST.....	17
FIGURE 2-9	Evolution Of The Variable Geometry Wing (Swing Wing).....	20
FIGURE 2-10	Evolution Of The Double Delta / Cranked Arrow Wing.....	22
FIGURE 2-11	Constraint Diagram.....	23
FIGURE 3-1	Supercruiser Wing Planform.....	24
FIGURE 3-2	Drag Polar.....	25
FIGURE 3-3	Change In $C_{L_{max}}$ Due to L.E. Flap Deflection....	27
FIGURE 3-4	Supercruiser L.E. Flap Placement.....	28
FIGURE 3-5	All Movable Vertical Tail.....	29
FIGURE 3-6	Vertical Tail With Rudder.....	29
FIGURE 3-7	Fuselage Configuration.....	31
FIGURE 3-8	Aircraft Cross Sectional Area Distribution.....	32

FIGURE 3-9	Final Drag Breakdown (Supersonic Cruise Condition).....	33
FIGURE 4-1	Inlet System: (a) External Compression System... (b) Internal Compression System...	38
FIGURE 5-1	A Comparison Of Composites And Metals By Specific Strength (Ultimate Tensile Strength / Density).....	42
FIGURE 5-2	A Comparison Of Composites And Metals By Specific Stiffness (Modulus / Density).....	42
FIGURE 5-3	Supercruiser Temperature Distribution (Mach 3.0).....	44
FIGURE 5-4	Fuselage Insulation Design	44
FIGURE 5-5	Wing Insulation Design.....	44
FIGURE 5-6	Graphite Polimide Laminate Schematic.....	46
FIGURE 5-7	Skin Panel Cross-Section.....	47
FIGURE 5-8	Spar And Rib Layout Of The Wing Section.....	47
FIGURE 5-9	Wing Deflection (3g Loading).....	49
FIGURE 6-1	Range As A Function Of $C_L^{1/2}/C_D$	55
FIGURE 6-2	Optimum Mach Number As A Function Of Altitude...	56
FIGURE 6-3	Endurance As A Function Of SFC.....	57
FIGURE 6-4	Effect Of $C_{L_{max}}$ On Landing Distance	58
FIGURE 8-1	Tri-Class Seating Arrangement.....	67
FIGURE 8-2	Cross Section Of The Fuselage.....	67
FIGURE 8-3	Location Of Access Doors / Emergency Slides.....	71
FIGURE 9-1	International Traffic Distribution.....	74
FIGURE 9-2	(a) Runway Fillet Requirement..... (b) Gate Parking.....	76
FIGURE 9-3	Servicing Vehicle Layout.....	76
FIGURE 9-4	Cost Comparison With Competitive Carriers.....	80

LIST OF TABLES

	Page
TABLE 3-1 Change In $C_{L_{max}}$ Due To Leading-Edge Flap Deflection.....	27
TABLE 3-2 Fuselage Drag Coefficients.....	31
TABLE 3-3 Total Aircraft Drag Breakdown Subsonic.....	32
TABLE 3-4 Total Aircraft Drag Breakdown Supersonic.....	33
TABLE 8-1 Number Of Facilities Located Within Each Class Section.....	70
TABLE 8-2 Number And Dimensions Of Access Doors.....	71
TABLE 9-1 Required Trucks And Other Servicing Vehicles,.....	77
TABLE 9-2 Cost Analysis Breakdown.....	78
TABLE 9-3 Operating Cost Per Block Hour.....	79

LIST OF SYMBOLS

AEA	Association Of European Airlines
$C_{D(i)}$	Induced Drag Coefficient
$C_{D(f)}$	Friction Drag Coefficient
$C_{D(total)}$	Total Drag Coefficient
$C_{D(wave)}$	Wave Drag Coefficient
DD/CA	Double Delta / Cranked Arrow
deg	Degrees
EPNdB	Effective Perceived Noise Level in Decibels
FAA	Federal Aviation Administration
FAR	Federal Aviation Regulations
FE	Finite Element
ft	Feet
ft/s	Feet Per Second
GE	General Electric
HS	High-Speed
HSCT	High-Speed Civil Transport
IVP	Inverted Velocity Profile
K	Conductivity Coefficient
L/D	Lift to Drag
L.E.	Leading Edge
M	Mach Number
MACQ	Manufacturing and Acquisition Cost
MD	McDonnell Douglas
n	Load Factor
NACA	National Advisory Committee on Aeronautics
NASA	National Aeronautics and Space Administration
nmi	Nautical Miles
NO_x	Oxides of Nitrogen (All Species)
OPS	Operating Cost
Po_c/Po_o	Total Pressure Recovery
P&W	Pratt and Whitney
rad	Radians
RDTE	Research, Development, Testing and Evaluation Cost
RFP	Request For Proposal
sec	Second
SERN	Single Expansion Ramp Nozzle
SST	Supersonic Transport
TBE	Turbine Bypass Engine
T/W	Trust Loading
USD	United States Dollars
VC	Variable Cycle
VCE	Variable Cycle Engine
VSCE	Variable-Stream Control Engine
VSOW	Variable Sweep Oblique-Wing
W_m	Natural Frequency
W/S	Wing Loading

Apogee Aeronautics Corporation

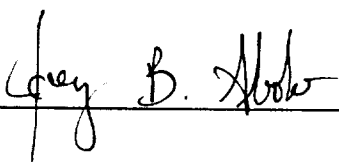
On December 17, 1903 at 10:35 A.M., the first sustained, controlled, powered flight of a heavier than air machine (The Wright Flyer I) was accomplished. This machine was constructed of spruce and cloth. Its empty weight was a 605 lb, its cruise velocity 10 ft/sec, and its range 120 ft. Since the first successful powered flight of the Wright Brothers, there have been many breakthroughs such as Charles Lindbergh's non-stop solo crossing of the Atlantic on May 20, 1927 and Charles "Chuck" Yeager's breaking of the sound barrier on October 14, 1947. Since the Wright Brothers first flight, it is apparent that man's intent has been to go farther and faster. A primary example is the current United States proposed research test bed, the X-30 National Aerospace Plane, which will have a proposed maximum speed of Mach 29 (almost 2000 times that of the Wright Flyer I).

The traditional concept of going farther and faster, is alive and well at Apogee Aeronautics Corporation. Our current project, a High-Speed Civil Transport (HSCT): designated the SUPERCRUISER, will uphold the tradition of record breaking aircraft. This second generation supersonic aircraft will fly faster and have a greater range than the first generation HSCT, the Concorde.

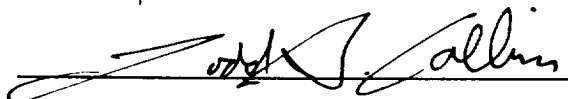
The traditions of quality engineering and the goal to push current technology to its limits is maintained at Apogee Aeronautics. It is in the spirit of these traditions that we present to you our design concept for the next generation HSCT: The Supercruiser Arrow HS - 8.

Respectfully:

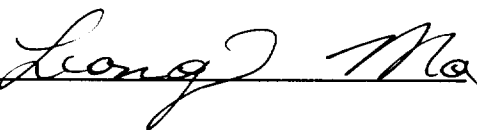
Joey B. Abobo

A handwritten signature in cursive script, reading "Joey B. Abobo", written over a horizontal line.

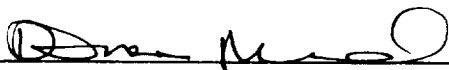
Todd A. Collins

A handwritten signature in cursive script, reading "Todd A. Collins", written over a horizontal line.

Leong Ma

A handwritten signature in cursive script, reading "Leong Ma", written over a horizontal line.

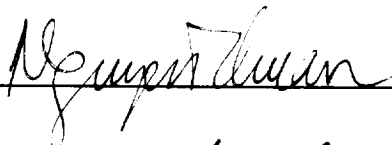
Adnan Murad

A handwritten signature in cursive script, reading "Adnan Murad", written over a horizontal line.

Hitesh Naran

A handwritten signature in cursive script, reading "Hitesh Naran", written over a horizontal line.

Thuan P. Nguyen

A handwritten signature in cursive script, reading "Thuan P. Nguyen", written over a horizontal line.

Timothy I. Nuon

A handwritten signature in cursive script, reading "Timothy I. Nuon", written over a horizontal line.

Dimitri D. Thomas

A handwritten signature in cursive script, reading "Dimitri D. Thomas", written over a horizontal line.

Executive Summary

This report discusses the design and marketability of a next generation supersonic transport. Apogee Aeronautics Corporation has designated its High Speed Civil Transport (HSCT): Supercruiser HS-8, which is shown in Figure i-1.

Since the beginning of the Concorde era, the general consensus has been that the proper time for the introduction of a next generation Supersonic Transport (SST) would depend upon the technical advances made in the areas of propulsion (reduction in emissions) and material composites (stronger, lighter materials). It is believed by many in the aerospace industry that these beforementioned technical advances lie on the horizon. With this being the case, this is the proper time to begin the design phase for the next generation HSCT.

The design objective for a HSCT was to develop an aircraft that would be capable of transporting at least 250 passengers with baggage at a distance of 5500 nmi. The supersonic Mach number is currently unspecified. In addition, the design had to be marketable, cost effective, and certifiable. To achieve this goal, technical advances in the current SSTs must be made, especially in the areas of aerodynamics and propulsion.

As a result of these required aerodynamic advances, several different supersonic design concepts were reviewed. Among these design concepts were the oblique wing, variable swing wing, and the double delta / cranked arrow (DD/CA) configuration. The DD/CA

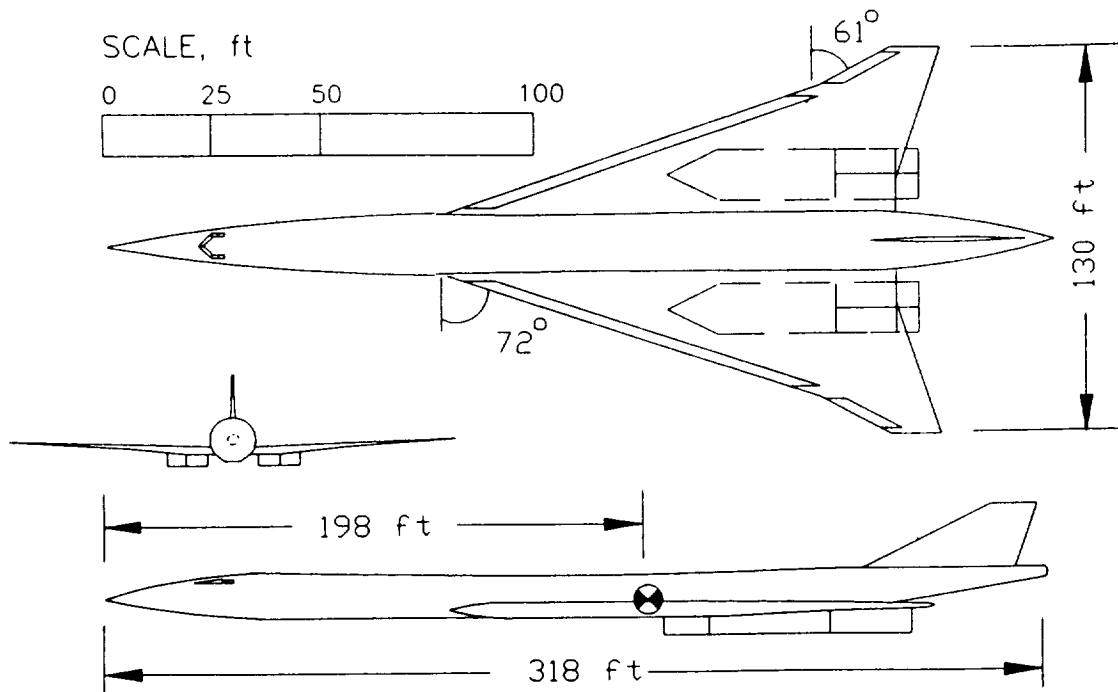


FIGURE i-1. Supercruiser HS - 8

configuration was chosen because it represented the best compromise between both supersonic and subsonic flight regimes while still maintaining its cost effectiveness. The variable swing wing concept represented the ultimate in aerodynamic efficiency for the two flight regimes, but offered increased cost along with other difficulties.

Due to the required propulsion system advances, several engines were reviewed. The possible candidates are as follows:

turbojet, turbofan, and variable cycle (VC) engines. Out of the three engine candidates, none had met the noise level requirements set by the Federal Aviation Administration (FAA): FAR Part 36, Stage 3. In addition, all current engine designs fail to provide the desired thrust and SFC combination required by an advanced HSCT aircraft. However, the best potential candidate to meet the FAA and HSCT requirements appeared to be the VC engine. As a result, research into improving this engine design is highly recommended by this study.

Advancement in material composites was determined to be a key parameter in the success of a HSCT. The studies conducted have indicated that a structure composed of composite materials would allow for a significant reduction of vehicle total weight (25 to 30 percent) without compromising the strength of the aircraft and without adversely affecting the vehicle cost. As a result of these significant weight savings, an all composite (approximately 85%) structure was incorporated into the Supercruiser.

The advanced technologies incorporated into the Supercruiser, along with its superior aerodynamics, allowed it to out perform the Concorde in passenger capacity (Supercruiser holds 300 passengers compared to Concorde's 144) while maintaining a comparable range (Supercruiser range with current engine technology is 3183 nmi compared to Concord's 3748). In addition to the Supercruiser's superior payload accommodations over the Concorde, the Supercruiser is also economically superior to the Concorde and comparable to the current subsonic fleet of transcontinental aircraft. The unit cost

of the Supercruiser is higher than that of its subsonic counterparts (Unit Price Per Supercruiser: 185 Million USD), however, economic analysis showed that the operating cost of the Supercruiser and its life cycle cost (LCC) are three times less than the competing subsonic carriers. If a range of 5500 nmi could be achieved (this is highly possible considering the current rate of propulsion and material composite advances), the profit range would be between 10% and 62%.

With the current growth trends in the Atlantic and Pacific Rim markets (growth potential of 27% and 53%, respectively), it is obvious that a next generation SST would be a profitable enterprise. It is for this reason that Apogee Aeronautics has begun the preliminary design phases of such an aircraft.

1.0 INTRODUCTION

1.1 Opportunity

The Concorde, a supersonic passenger transport resulting from the joint efforts of the British Aircraft Corporation and the French Aerospatiale, flew for the first time on March 2, 1969. It was a monumental technical achievement, however, economically it proved to be a tremendous failure. Because the Concorde was designed and built under a joint effort, it was saved several times by the "no cancellation clause" introduced by the two companies.

The obstacles facing the SST (Supersonic Transport) in 1969 were mainly economical and environmental. Due to the sonic boom it generated, the SST was banned from overland flight in the North America. This failure to achieve the rights to fly supersonically overland severely limited the market for the SST. The reduced market threatened to make the SST an economically unviable aircraft. In lieu of this economic threat, the development of the SST in the United States and the flight testing in Europe continued. The final blow was dealt to the United States' SST effort, when in 1971 the Federal Aviation Administration (FAA) introduced new laws that required lower Nitric Oxide emissions and lower maximum decibel levels for the engines of future civilian transports (The Concorde survived because it went into production before the new law was enacted). The ability to limit the noise and emission levels to those values dictated by the FAA were not possible with the technology available. Thus as a result of this

new legislation, the Boeing SST project was cancelled in 1971.

One basic lesson from the evolution of air transport technology, that was true at the beginning of the SST era and which is still true today, is that increased speed and increased capacity (ie. lower fares) spells success*. Therefore, the proper time for the introduction of the next generation SST will depend upon the technical advances made in the aerospace field. It is the general consensus that the required advances in engine design and material technology lie on the horizon. This being the case, it is the proper time to begin the design phases for the second generation SST.

* The Concorde failed to meet the increased capacity criterion; its passenger capabilities being about a third of its chief competitor, the Boeing 747.

1.2 Request For Proposal (RFP)

The request for proposal (RFP) supplied to Apogee Aeronautics Corporation by the 1991-92 Aerospace HSCT Design Board at California State Polytechnic University, Pomona (referred to from here on as RFP 1A), was quite general in its specifications. As a result, the corporation also decided to consider the requirements proposed by the Association of European Airlines (AEA). The AEA's RFP, 'General Requirements For Future High Speed Commercial Transports', will be referred to from here on as RFP 1B. In the interest of the reader, RFP 1A will be presented in its entirety, while the pertinent design criterion not mentioned in RFP 1A will be summarized from RFP 1B.

1.2.1 RFP 1A

Project Objective

The objective is the design of a High Speed Civil Transport aircraft for entry into the market place under full production of 500 aircraft. Cost reduction and certification of the design are key objectives that will require careful consideration of available technology and its risks. Tradeoff studies in aircraft speed, capacity, cargo flexibility, and range must be made.

The new supersonic transport aircraft must be affordable and marketable. This aircraft will cost more than the current production aircraft on a cost basis, but the aircraft will offer superb speed advantages and a significant increase in performance. The aircraft must appeal to the airlines and a production fleet of 500 aircrafts will be assumed. A production fleet under 500 units will be uneconomical for both the airframe manufacturer and the airlines. Upgrade paths will also be considered.

The aircraft is intended to be used in long range flights so it must be safe, simple to fly, and require minimal maintenance. Furthermore, this aircraft should require minimal personnel conversion training in both operation and maintenance.

The aircraft must minimize environmental impact, especially in the area of sonic boom over-pressure. This aircraft must meet FAA certification criterion of FAR Part 25. In addition, this aircraft must be able to be certified and fit in with the current designs in both the air-traffic system and in the ground support system. A safety factor of 1.5 must be incorporated into the design.

Requirements

Design Mission

1. Payload is for a minimum of 250 passengers with baggage
2. Warm-up, taxi, and takeoff from sea level runway
3. Climb on cruise to best altitude
4. Cruise to a point 6500 nmi from takeoff
5. Descend on course to sea level
6. Landing
7. Reserves

Performance

1. Level Cruise Mach number?
2. The cabin floor angle shall not exceed 2 deg during normal cruise
3. Satisfy second stage climb requirements (off design performance)
4. Takeoff and land from 10,000 ft runway with 50 ft obstacle

Supportability

To remain profitable, an airline must be able to utilize its aircraft around the clock throughout its useful life. Admitting that corrosion, wear, and aging degrades an airplane; the aircraft must be easily inspectable. If a critical part is discovered, it must be available to the mechanic and easily replaced.

Certification

The aircraft must meet standards, rules, and regulations pertinent to the design of this class of aircraft in FAR Part 25.

Data Requirements

The proposal, based on the previously stated objectives, requirements, and constraints, should substantiate the following:

1. Justify the design. Include a discussion of the design tradeoff studies that were performed to arrive at the proposed design. Present the performance, maintainability and reliability (M & R), and cost criteria by which the final design was chosen. Include the sizing trade study results to show how the pertinent aircraft parameters were chosen (aspect ratio, taper ratio, airfoil thickness, engine size, etc). Describe the anticipated changes in these parameters if the performance requirements are modified.

2. A full set of drawings that depict the design must be provided. This will include, but is not limited to: a) A three view drawing with appropriate dimensions. b) An internal layout to show seating arrangements. c) A system integration drawing that shows the location of flight critical systems such as flight controls. d) A cockpit layout that shows the instrument panel and the controls.

3. The structural design, including materials, and the method of determining the structural strength should be described. The weight and balance data must be tabulated and the center of gravity and its travel indicated on the three-view drawing. Load diagrams with tip-over angles and stability limits must be included.

4. Describe the methods and the results of the evaluations of performance, stability and control, and handling qualities of the proposed design. The design of the control system should be provided.

5. Maintainability and Reliability. Features of the aircraft that improve the M & R of the aircraft should be explained.

6. Acquisition and Operating Cost. A breakdown of the manufacturing cost, the cost of ownership, the direct operating cost and the indirect operating cost should be reported for the useful life span of the aircraft. The methods and assumptions used to arrive at these results are equally important for accurate comparison to competing designs.

7. Engine Data. An engine will be provided for this proposal. The proposer has the option to substitute any available propulsion data with the provision that it be adequately substantiated to show viability.

1.2.2 RFP 1B

The AEA recommendations which are relevant to this stage of aircraft development which have not been stated in RFP 1A will be stated below:

General

1. The aircraft must be designed to serve all the levels of business travelers, not excluding the tourist traveler.
2. For economic flexibility to the operation, economy class, freight and mail will be contemplated as secondary products.

Capacity and Payload Accommodations

1. The aircraft must carry a minimum of 250 passengers.
2. The fundamental issue for this aircraft will be interior flexibility.
3. There must be at least the provision for three galley areas.
4. Cabin floor attitude in cruise flight must not exceed 2 deg.
5. Belly compartments must be compatible with the LD-3 base design.

Crew Accommodations

1. Certified for a cockpit of two members.
2. Two observer seats will be provided in the cockpit.
3. Cockpit external visibility will fulfill the international rules at the time of production.
4. Special attention shall be given to the comfort and protection of the crew, in particular to noise (levels and quality), vibrations, climatisation, and radiation protection.

Operational Requirements

1. Turnaround time of 2 hours at main base, and within 1 hour at stations, is required.

Environmental Requirements

1. Emissions must meet any regulatory requirement at the time of service and be at levels that would not impose local operation restrictions. Engine emissions should be reduced to a level that would not endanger the atmosphere.

Airframe and Systems Design

1. The main structure should be designed and tested for a fatigue life of not less than 75,000 flight hours and 25,000 cycles.

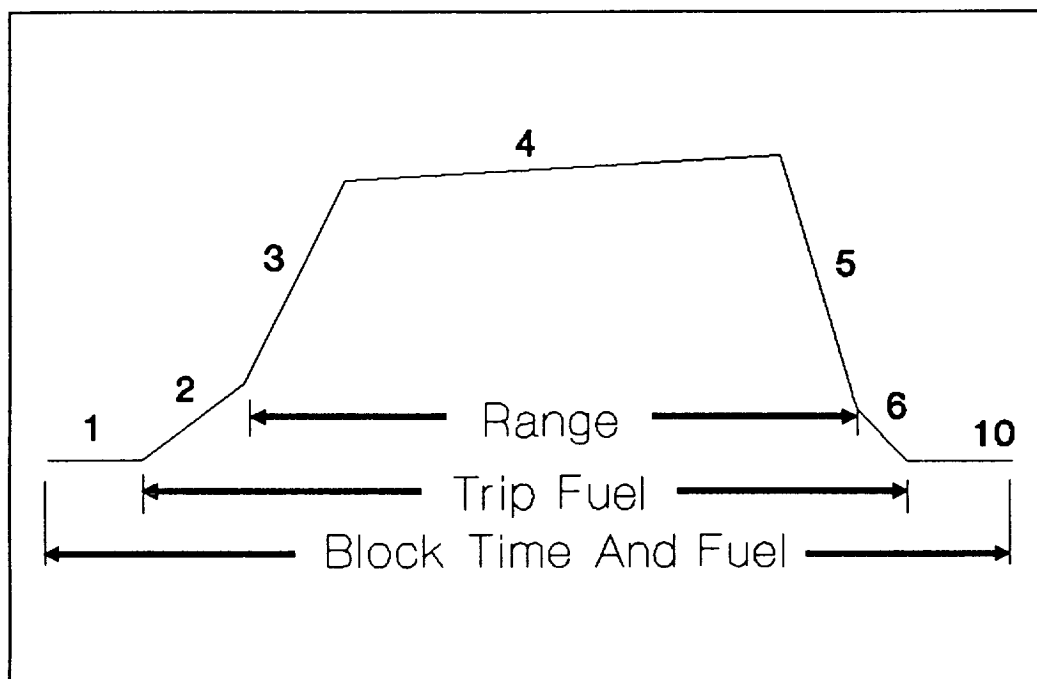
Propulsion Design

1. The engines should be designed to be operated with standard jet fuel.

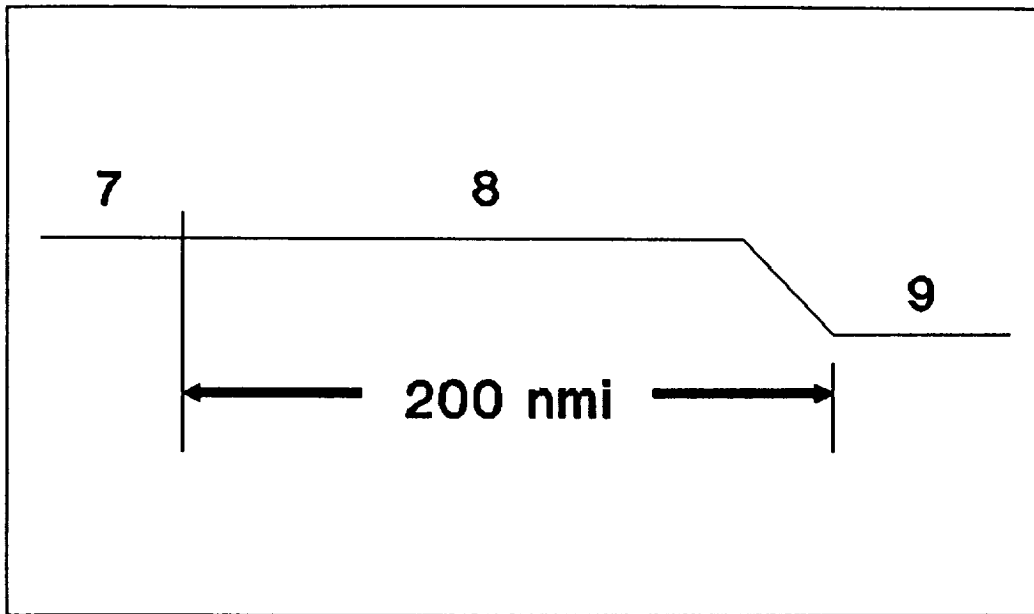
1.3 Flight Profile

The following are the baseline parameters for a flight profile of a supersonic transport as determined by the RFP. Figure 1-1 illustrates this graphically.

1. 15 Minute Warmup And Taxi-Out
2. 2 Minute Takeoff
3. Accelerate/Climb
4. Supersonic Climbing Cruise
5. Descend/Decelerate
6. 4 Minute Approach
7. 6 % Trip Fuel
8. Subsonic Cruise At 30,000 ft
9. 30 Minute Hold At Selected Altitude
10. 6 Minute Taxi-In



(a)



(b)

FIGURE 1-1. Flight Profile: (a) Routine Mission Profile
(b) Alternate Airport Selection

2.0 VEHICLE DEVELOPMENT

2.1 Vehicle Concepts

A considerable amount of the aeronautical research conducted by the National Aeronautics and Space Administration (NASA) has been devoted to the problems associated with the ability of man to fly at supersonic speeds up to four times the speed of sound. The purpose of this research was to develop a technology base in which U.S. military services and the American aerospace industry could take advantage of when considering the viability of high-speed manned flight. In concert with the research conducted by NASA, Apogee Aeronautics focused its efforts on the feasibility of a long-range, High-Speed Civil Transport (HSCT) aircraft that would be affordable and marketable when introduced into the marketplace. Thus, various vehicle concepts were considered in order to determine which concepts are viable.

At Apogee Aeronautics, our first consideration was the type of fuselage needed in order to meet the RFP requirements. With this in mind, four fuselages were considered: cylindrical, twin-fuselage, blended wing-body, and oblique flying wing. A comparison of the practicability of these configurations in the marketplace was considered along with market acceptability (ie. mainstream thinking). The second consideration was what type of particular wing configuration would optimize the HSCT performance in subsonic, transonic, and supersonic regimes. Various wing configurations that are applicable to subsonic and supersonic flight were

investigated. There are primarily four wing configurations that have been considered the most practical in a HSCT aircraft. These four wing configurations are: fixed swept, variable sweep, double delta/cranked arrow (DD/CA), and variable sweep oblique-wings. These four wing designs have been experimentally tested in the realm of supersonic cruise flight and have been proposed as a viable design feature for our HSCT program.

2.1.1 Fuselage Design Configurations

The first design configuration to be considered is the cylindrical fuselage. This configuration is a cylindrical tube streamlined for supersonic flight. An approximate representation of the this type of fuselage is shown in Figure 2-1. This configuration represents mainstream thinking, since the bulk of all civil transport aircraft incorporate the cylindrical fuselage. The cylindrical fuselage configuration can be altered in order to accommodate the payload without constraining space availability to its occupants.

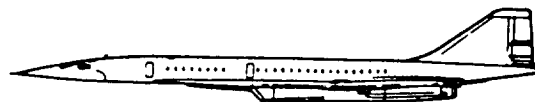


FIGURE 2-1. Cylindrical Fuselage Configurations: Tupolev Tu-144 "Charger"

The fuselage is streamlined in order to keep aerodynamic drag reasonably low.

Another fuselage configuration considered is the twin-fuselage represented in Figure 2-2. In order for our HSCT aircraft to be economical, it has to maximize its passenger payload while reducing flight cost. Therefore, the twin-fuselage was proposed in order to meet the increased passenger demand while minimizing cost. An attractive feature of this fuselage concept is an increase in volume could be obtained at little cost in aerodynamic efficiency. In other words, the integration of two fuselages connected by various lifting and control

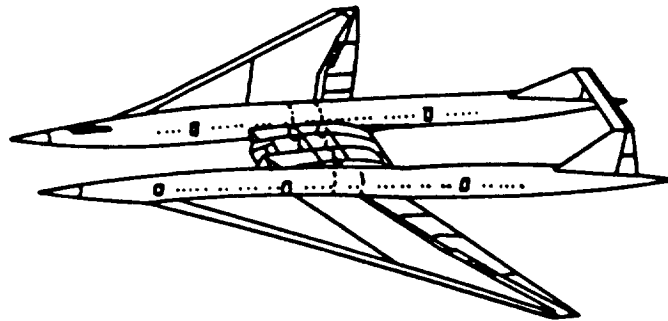


FIGURE 2-2. Proposed Large-Payload, Twin-Fuselage SST

surfaces would not significantly effect the aerodynamic efficiency of the aircraft.

The two fuselages are almost identical to the cylindrical type fuselage mentioned above. Instead of having one fuselage, two fuselages are incorporated. All the same features included in the cylindrical fuselage configuration are represented in the twin-fuselage configuration.

The third fuselage configuration to be considered is the blended wing-body configuration shown in Figure 2-3. This particular configuration integrates both the fuselage and wing into one composite body. The draw back to this body configuration is its limited flexibility and lack of proven technology.

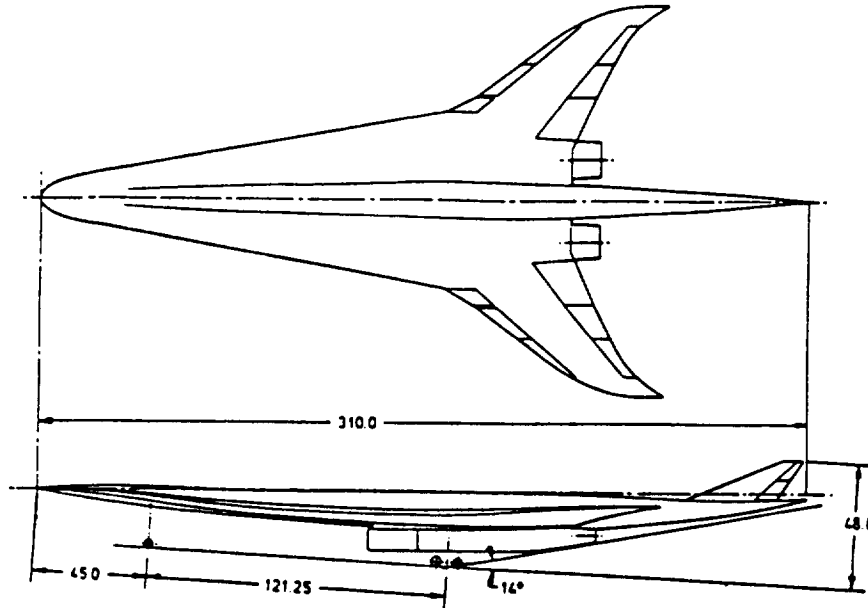


FIGURE 2-3. Proposed Blended Wing-Body Arrangement Where Dimensions Are Given In Feet, Except As Noted

The final fuselage configuration to be considered is the oblique flying wing as shown in Figure 2-4. This aircraft/fuselage design combination is the brainchild of R.T. Jones. It essentially represents a configuration that lacks the conventional appearance of a commercial aircraft, but has the capability to transport approximately 500 passengers at speeds approaching Mach 1.5.

Unlike the other fuselages, the oblique flying wing is genuinely aerodynamically efficient. An important note to consider is the fuel placement in the oblique wing, since it does not meet

FAA regulations. Another feature of this configuration is the fact that at supersonic speeds the absence of a fuselage would effectively lower the amount of surface area exposed; thus reducing wave drag. These attributes could make the oblique wing economical if introduced into the supersonic transport marketplace.

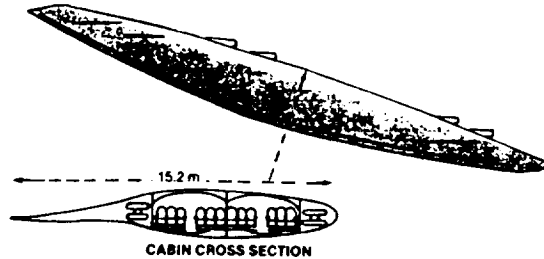


FIGURE 2-4. Oblique Wing Configuration

2.1.2 Wing Design Configurations

The first wing configuration design considered was the fixed swept wing. This configuration, shown in Figure 2-5, is similar to the conventional wing designs of large commercial transports such as the 747 and MD-12. It does not drastically deviate from the standard wing configurations currently being produced by various aerospace companies. The combination of the dual cylindrical fuselage and fixed swept wing configuration theoretically has the ability to produce a HSCT with a lift-to-drag ratio at cruise of 8.1 at approximately Mach 2.6. Even though this wing configuration proves to be sufficient at supersonic speeds, it does have its disadvantages when flying at subsonic and transonic speeds. Since highly swept wings are designed for supersonic flight, they require a high thrust load in order to maintain sufficient subsonic cruise. This compromises the fuel efficiency and the range of the aircraft.

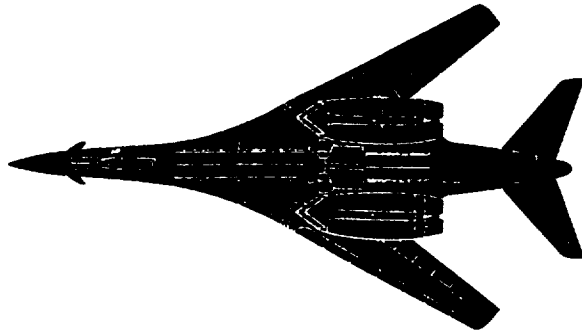


FIGURE 2-5. Fixed Swept Wing Configuration

Current sonic boom restrictions require that an SST be aerodynamically efficient in both the subsonic and supersonic regions. Thus modifications to the design of the fixed wing would be required to improve subsonic aerodynamics in order to make such a proposal viable for Apogee Aeronautics and economical for the HSCT passengers.

In order to compensate for the low aerodynamic performance characteristics of the fixed swept wing in subsonic flight, a variable sweep wing configuration was considered. This configuration, shown in Figure 2-6, is similar to the fixed swept wing except when at subsonic speeds, the wings are extended outward thus reducing the thrust load required to maintain the aircraft in flight.

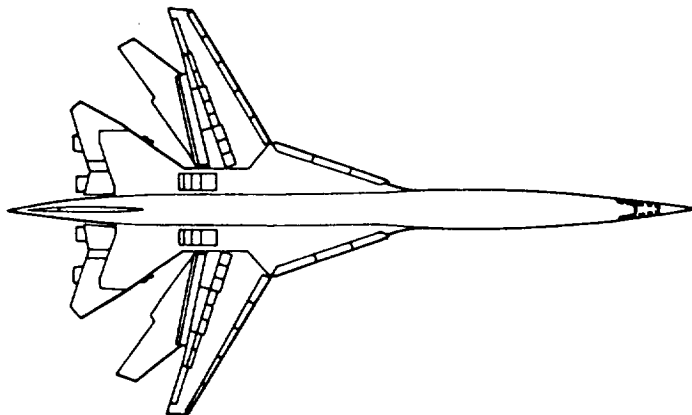


FIGURE 2-6. Variable Sweep Wing Configuration

The variable sweep wing provides the same L/D ratio at cruise as the fixed swept wing at supersonic speeds, but with less fuel expenditure to arrive at supersonic cruise conditions. The variable sweep wing, because of its ability to extend and retract, features flexibility of operation with optimization of aerodynamic performance throughout all flight regimes. This particular feature of the variable sweep wing enables the aircraft to maintain aerodynamic efficiency while meeting the rigorous economical demands of fuel cost and other related expenditures.

The third wing configuration to be considered for the HSCT program is the double delta/cranked arrow (DD/CA) wing configuration, as shown in Figure 2-7.

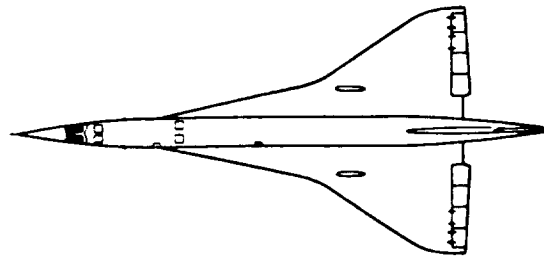


FIGURE 2-7. Double Delta/Cranked Arrow Type Configurations: Tupolev Tu-144 "Charger"

This configuration takes advantage of the physical and aerodynamic characteristics of the fixed swept and variable sweep wing designs. The DD/CA wing was shown to have a cruise L/D ratio of 10.0, while maintaining a superior supersonic L/D (approximately 7.5). This demonstrates that this wing configuration is comparable to the fixed swept and variable sweep wing configurations in aerodynamic efficiency; thus making it the preferred selection over the previous wing configurations mentioned.

2.2 Initial Configurations

The RFP requested that a major priority be given to the reduction of the sonic boom over-pressure such that the aircraft could maintain supersonic flight overland and populated areas. However, knowing that the possibility of achieving acceptable over-pressure levels was not likely to happen, the RFP had a provision for a mixed flight envelope consisting of supersonic and subsonic phases. The nature of the mixed flight regime immediately set the criteria for the selection of the initial configurations. This criteria required that the aircraft have a good performance in both the subsonic and supersonic flight regimes. Out of the initial configurations there were only three which offered the desired supersonic and subsonic aerodynamic qualities. These three initial configurations are the Oblique Wing, Double Delta / Cranked Arrow, and the Swing Wing.

2.2.1 Oblique Wing

The oblique wing offered excellent subsonic and low Mach number supersonic characteristics. However, with the selection of the oblique wing came the selection of the unknown. Light, one man oblique wing test-bed aircraft are being flown by NASA to demonstrate the configurations aerodynamic superiority. But the applicability of this data to larger commercial transport versions is uncertain. Also, there is uncertainty in the reliability of the Oblique wings central pivot mechanism. Furthermore, there is uncertainty as to whether or not the public would accept an

unconventional configuration such as the Oblique wing. As a result of the above uncertainties, the Oblique wing concept did not proceed past the initial configuration stage.

2.2.2 Swing Wing

Figure 2-9 shows the evolution of the variable geometry wing (swing wing) as it survived the initial design phase for a number of reasons. The first and most important reason, as mentioned above, was that the swing wing was seen as the ultimate method of reducing the amount of aerodynamic compromise that existed between the supersonic and subsonic flight regimes. With the wings fully extended (aspect ratio of 8.31) it could enjoy the aerodynamic characteristics of a subsonic aircraft such as lower landing speeds and less induced drag. For the supersonic flight regime, the swing wing could reduce its aspect ratio to 2.17 with the wings fully swept. In this configuration, the aircraft would have less wave drag, thus reducing the required full load for the mission. Like the oblique wing, the swing wing design would be a first for a commercial transport. However, the swing wing, unlike the oblique wing, has been used in several military aircraft (the B1-B and the F-14 are just two examples). Therefore, it is more likely that this untraditional design would be seen as an application of the newest technology instead of the application of unproven technology. With the exception of its variable geometry system, the swing wing would have structures similar to those of the current subsonic aircraft (ie. two straight spars running from root

to tip; in contrast to the double delta which requires a bent spar for the outboard portion of the wing). As a result, the fabrication process for the wing would be similar to the process existing for the current subsonic carriers.

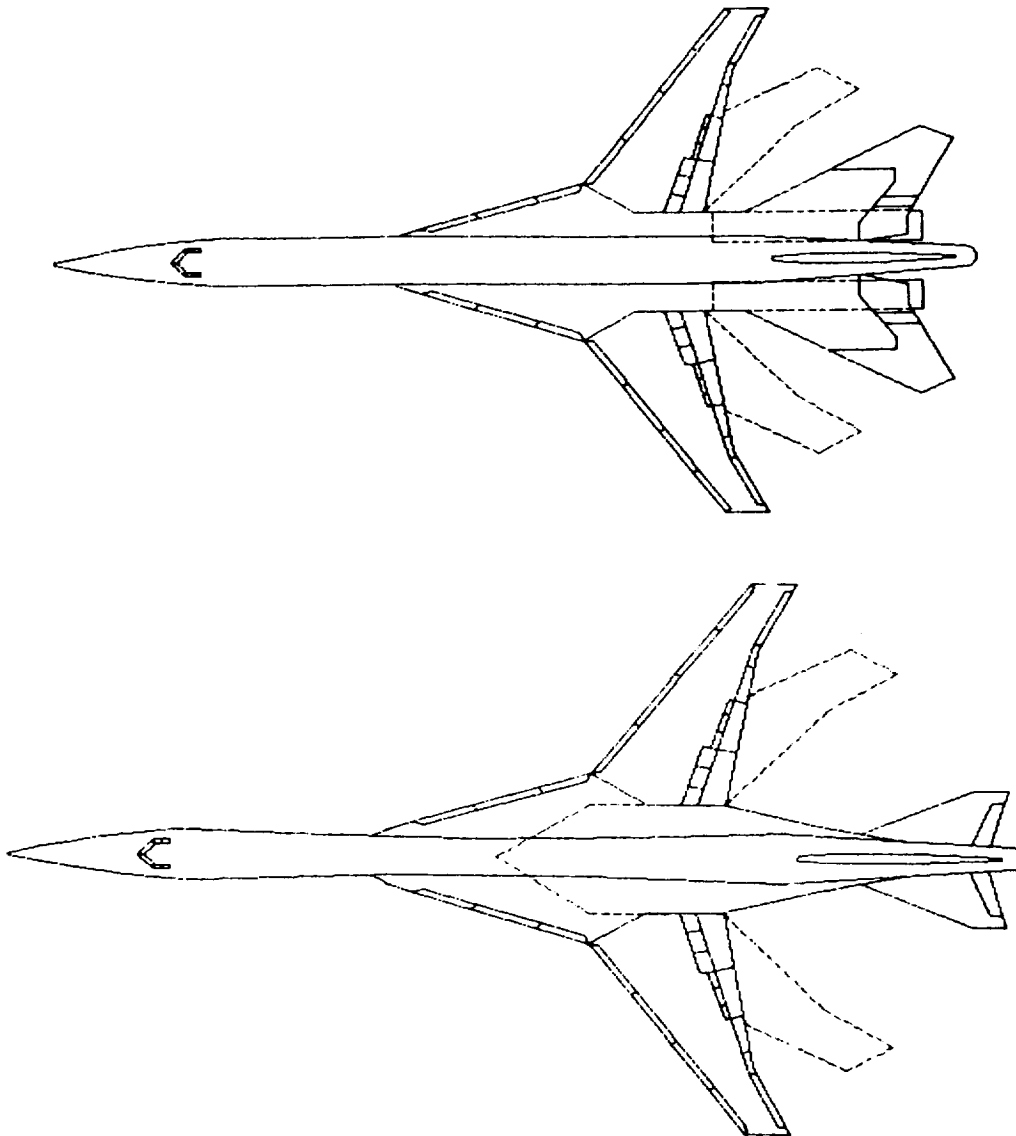


FIGURE 2-9. Evolution Of The Variable Geometry Wing (Swing Wing)

Even though the variable sweep wing appears to be the ideal wing configuration, it is unfortunately not immune to the disadvantages of its design. Due to the complexity of the mechanisms constituting the variable sweep wing, this variable sweep feature poses structural design and weight problems of uncertain proportions. The potential application of the variable sweep wing configuration for a HSCT was basically shelved in lieu of other proposed developments in wing configurations with less complexity, structural and weight problems.

2.2.3 Double Delta/Cranked Arrow Wing (DD/CA)

Figure 2-10 shows the evolution of the DD/CA configuration as it survived the first phase of the design process. Like the swing wing, the DD/CA configuration offered good subsonic and supersonic characteristics. This optimum balance between the two flight regimes is achieved by the breaking of the wing into a region which falls within the supersonic Mach cone and a region which is not encompassed by the Mach cone. The region which is not encompassed by the Mach cone allows for better subsonic performance, since it has less sweep (ie. greater aspect ratio). The inverse is true for the inboard portion of the wing. In addition to the favorable aerodynamic qualities of the DD/CA configuration, the wing is also capable of carrying a large amount of fuel. Thus the DD/CA was chosen to be the final configuration for the Supercruiser.

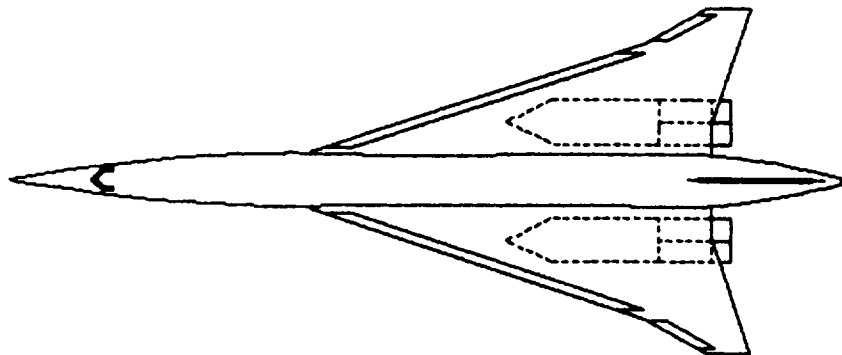
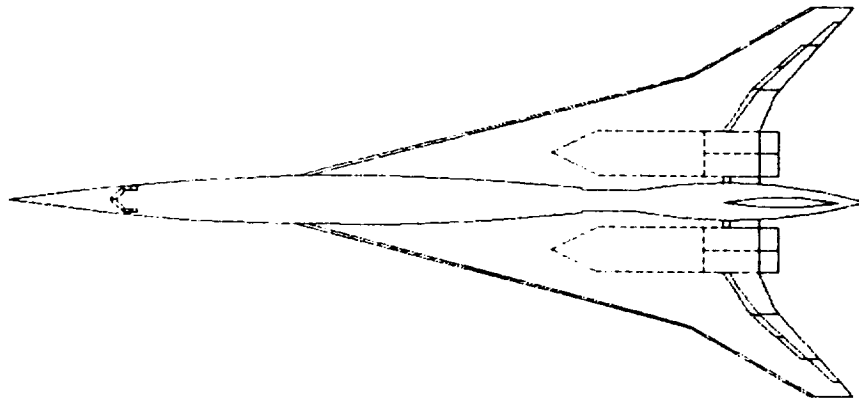
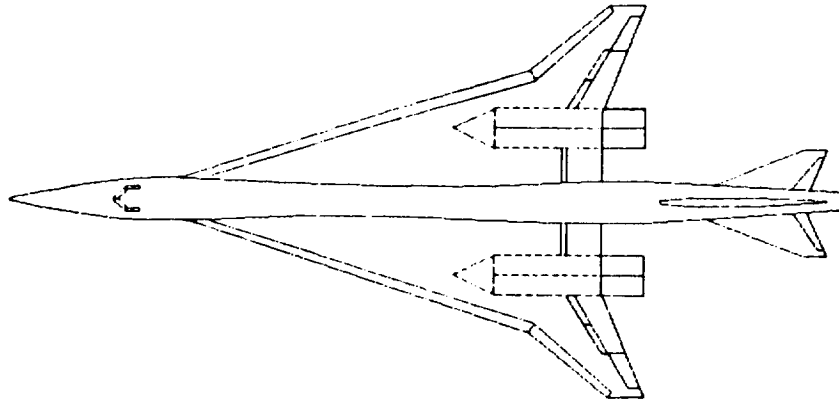


FIGURE 2-10. Evolution Of The Double-Delta Arrow Wing

2.3 Constraint Diagram

The following parameters were incorporated into the formulation of the constraint diagram for the Supercruiser.

Range: 6,500 nmi
Rate Of Climb: 89 ft/s
Takeoff Distance: 10,000 ft
Landing Distance: 10,000 ft
Cruise Speed: Mach 3.0

The resulting constraint diagram is shown in Figure 2-11. The figure shows that the optimum range for the thrust loading is: $23 < W/S < 104$ and the optimum range for the thrust to weight ratio is: $0.4 < T/W < 1.3$. Apogee Aeronautics' aircraft design was limited by the available technology. As a result, the Supercruiser has a $T/W=0.3$ and a $W/S=110$.

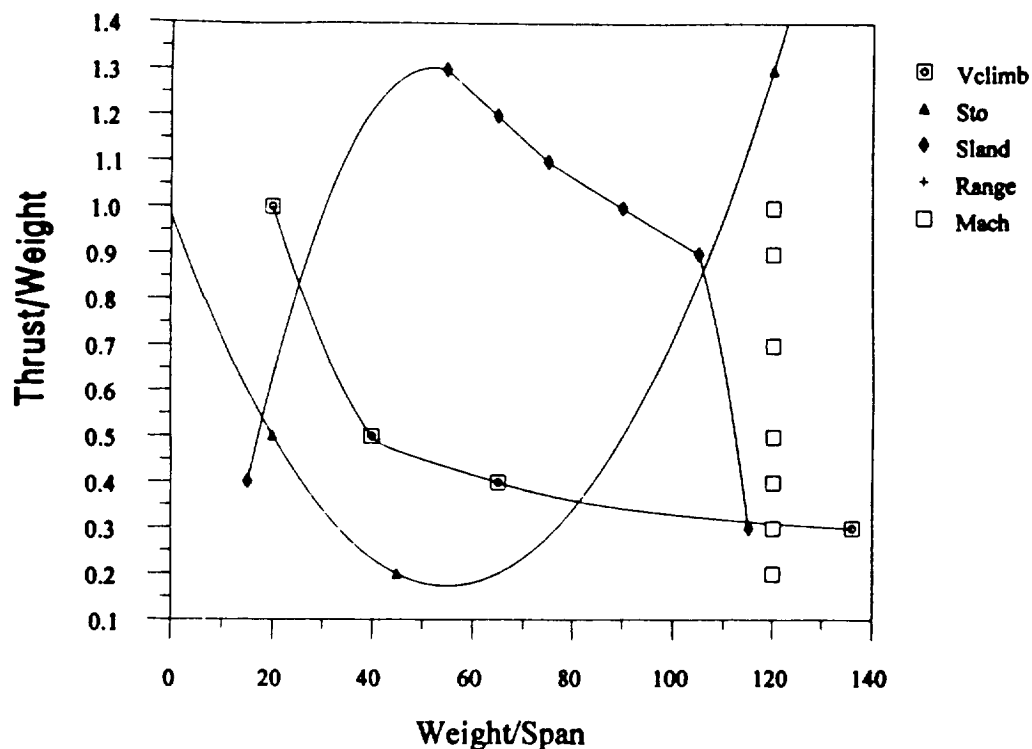


FIGURE 2-11. Constraint Diagram

3.0 AERODYNAMICS

3.1 Wing Design

Compromise between adequate structural integrity and aerodynamics effectiveness is required for a supersonic airfoil. With these compromises in mind, the airfoil selected for the Supercruiser is a modified NACA 65-006. The modification being a max thickness to chord ratio of 3 percent. For the NACA 65-006, the maximum thickness is near the aerodynamic center, thus allowing the main spar to be right at the region of maximum loading.

The double delta wing planform of the Supercruiser is shown in Figure 3-1. The span of the wing is 130 feet with a total planform area of 10,000 ft². The aspect ratio and the inner and outer wing taper ratios are 1.69, 0.28, and 0.25, respectively.

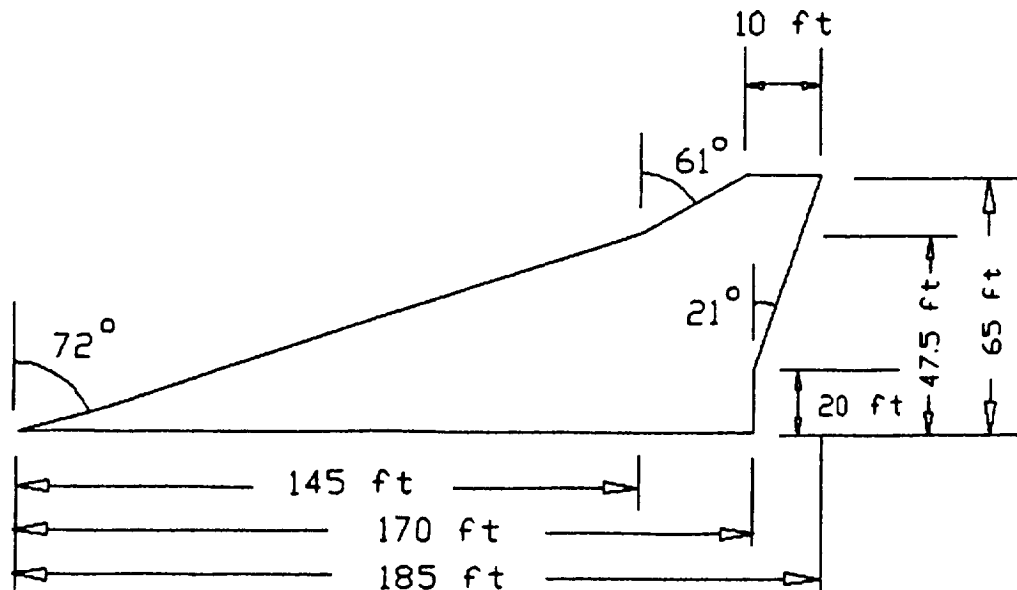


FIGURE 3-1. Wing Planform For The Supercruiser

The inboard leading edge of the wing is swept back 72 deg. so that the inboard section of the wing is within the Mach cone. The subsonic flow normal to the leading edge allowed the Supercruiser to use a rounded leading edge over the inboard section of the wing (this improves the aerodynamic efficiency) without substantial drag penalties. The outboard leading edge is swept back 61 deg. Since this portion of the wing experiences supersonic flow normal to the leading edge, a sharp leading edge airfoil was selected to minimize wave drag.

Utilizing the above planform, the drag polar for the wing was produced for the subsonic and supersonic flight regimes. The drag polar is shown in Figure 3-2.

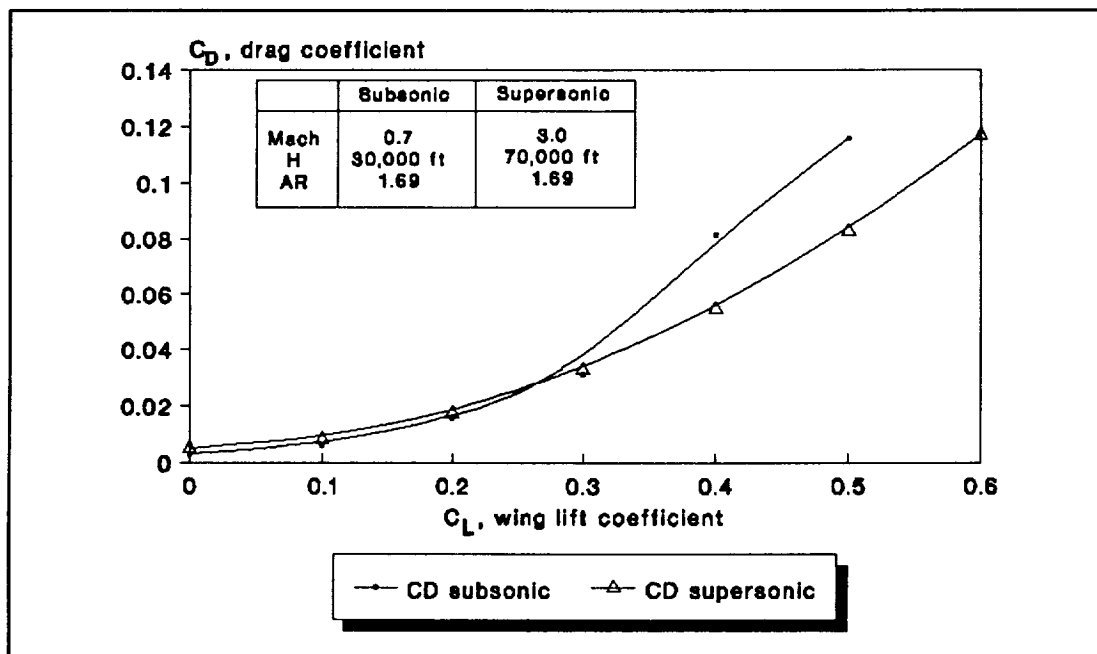


FIGURE 3-2. Drag Polar

3.2 High Lift Devices

In order for the Supercruiser to have superior takeoff and landing performances, high lift devices such as trailing-edge flaps and leading-edge flaps were considered. The Arrow HS - 8 configuration has been fitted with full-span leading-edge flaps, to improve, primarily, the takeoff performance of the aircraft.

3.2.1 Trailing-Edge Flaps

The analysis performed for the Supercruiser configured with trailing-edge flaps showed that the flaps slightly promoted flow separation due to the increase in upwash at the leading edge. Wing sweep promotes stall, and trailing-edge flaps become practically ineffective on wings that are swept past 35 deg. As a result of the previously mentioned short falls, trailing-edge flaps were not considered for the Supercruiser.

3.2.2 Leading-Edge Flaps

With the facilities currently being utilized, only experimental and statistical data was used to predict the change in $(C_L)_{\max}$ for a wing with leading-edge devices. The computed values for the change in $(C_L)_{\max}$ due to leading-edge flap deflection is given in Table 3-1 and is shown graphically in Figure 3-3. The placement of leading-edge-flaps are also shown in Figure 3-10.

TABLE 3-1

Change In $(C_L)_{\max}$ Due To Leading Edge-Flap Deflection.

Deflection (deg)	Change in $C(L)_{\max}$
10	0.4329
15	0.6023
20	0.6778
25	0.7338
30	0.7594
35	0.7908
40	0.8284
45	0.8660
50	0.8660
55	0.8724
60	0.8724

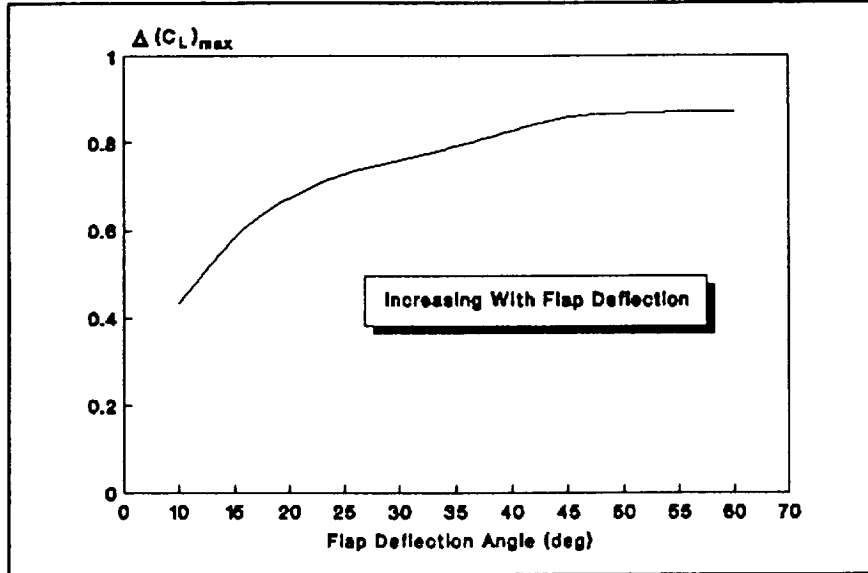


FIGURE 3-3. Change In $(C_L)_{\max}$ Due To L.E. Flap Deflection

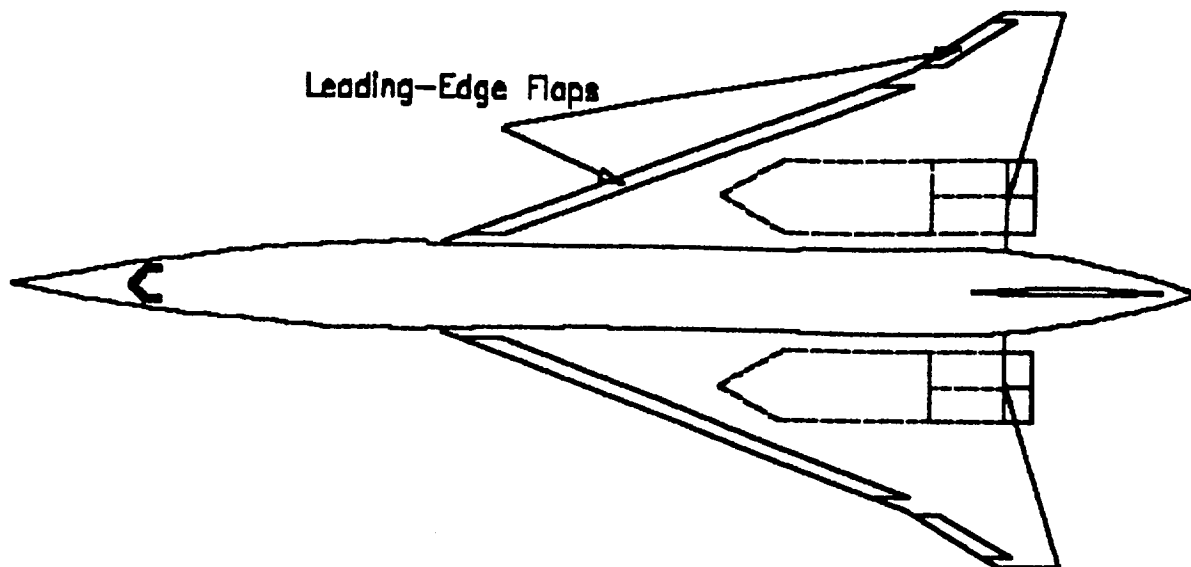


FIGURE 3-4. L.E. Flap Placement On The Supercruiser

The leading-edge flaps are able to achieve the desired $(C_L)_{\max}$ at landing and takeoff. Therefore, due to limiting the complexity of the wing while still maintaining adequate lift and control of the Supercruiser, the trailing-edge flaps were dropped from the final design configuration.

3.3 Vertical Tail Design

Two vertical tail concepts were considered for the Supercruiser's lateral-directional control. An all-movable vertical tail and vertical tail with rudder. Control about the lateral-directional axis is sensitive to changes in Mach number, dynamic pressure, and load factor. This sensitivity is due to strong nonlinearities in key stability derivatives and considerable reductions of control effectiveness caused by structural flexibility. The geometries of the two tail designs are shown in Figures 3-5 and 3-6.

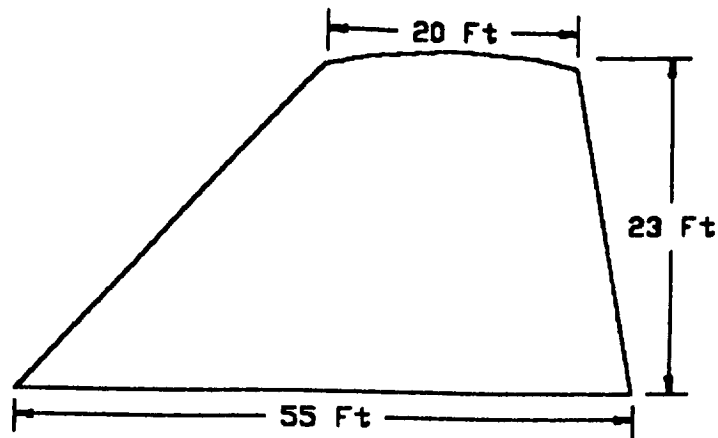


FIGURE 3-5. All-Movable Vertical Tail

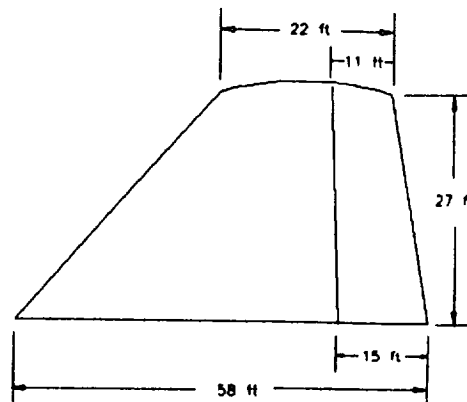


FIGURE 3-6. Vertical Tail With Rudder

Using stability computer simulation, the Supercruiser's stability behavior was analyzed for the all-movable vertical tail and the vertical tail with rudder. The results for both vertical tails are shown below.

ALL-MOVABLE VERTICAL TAIL

DUTCH ROLL MODE

Frequency (rad/sec)	0.24
Damped freq. (rad/sec)	0.14
Damping ratio	-.80
Period (sec)	26.71
Time to damp (sec)	-3.66
Flying Quality	Level 3

VERTICAL TAIL WITH RUDDER

DUTCH ROLL MODE

Frequency (rad/sec)	0.56
Damped freq. (rad/sec)	0.56
Damping ratio	-0.15
Period (sec)	11.17
Time to damp (sec)	-8.42
Flying quality	Level 3

SPIRAL MODE

Time constant (sec)	21.48
Flying quality	Level 2

ROLL MODE

Time constant (sec)	1.45
Flying quality	Level 2

SPIRAL MODE

Time constant (sec)	65.85
Flying quality	Level 1

ROLL MODE

Time constant (sec)	1.86
Flying quality	Level 2

Dynamically, the vertical tail with rudder was preferred because higher flight quality was achieved for the spiral mode. However, the magnitude of the lateral force generated on the tail is proportional to flight speed and it was calculated to be 13,700 lb at Mach 3.0. This force, which is acting only on the rudder area, could twist the tail structure to a point where it would fail. Therefore, it was determined that the Supercruiser would utilize the all-movable vertical tail as its vertical stabilizer.

3.4 Fuselage Design

One of the primary drivers in the fuselage design was its ability to accommodate for 275+ passengers including baggage. With this RFP requirement in mind, a payload of 300 passengers including baggage was considered. The length of the fuselage and its maximum diameter was determined using the following parameters: ability to accommodate for 300 passengers including baggage, flight deck, and required facilities and systems to properly maintain the aircraft. The beforementioned parameters resulted in a fuselage length of 318 ft and a maximum diameter of 17.1 ft.

Utilizing area ruling and wave-drag computer simulation, the fuselage's diameter was varied according to longitudinal location. This was done in order to optimize its performance in the supersonic flight regime. Figure 3-7 shows the final configuration of the fuselage excluding the vertical tail and the wings. In order to determine the fuselage's impact on the overall performance of the aircraft, the fuselage drag coefficient was evaluated at three different stages, as shown in Table 3-2.

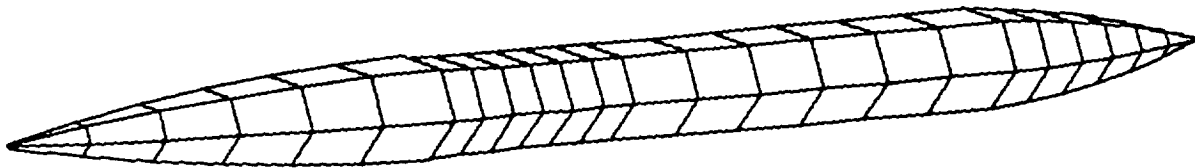


FIGURE 3-7 The Supercruiser's Fuselage Configuration

TABLE 3-2
Fuselage Drag Coefficients

Mach Number	Altitude (ft)	Drag Coefficient
0.7	30,000	0.00205
0.8 < M < 1.2	30,000	0.00706
3.0	70,000	0.00602

The drag coefficients of the fuselage evaluated at three different Mach regimes are comparable to those of current supersonic aircraft. This indicates that our chosen fuselage configuration is aerodynamically sufficient.

3.5 Total Aircraft Drag

The initial total drag breakdown for the aircraft at the supersonic cruise condition (Mach 3.0) is shown in Table 3-3. The highest drag contributor is the wave drag. Wave drag accounted for 52 percent of the total drag, while friction and induced drag accounted for 23 and 25 percent of the total drag, respectively.

Table 3-3
Total Aircraft Drag Breakdown
(Supersonic)

	M = 3.0 Wing	H = 70,000 ft Fuselage	AR = 1.69 Tail
$C_{D(\text{total})}$	0.00955	0.00620	0.001800
$C_{D(f)}$	0.00280	0.00014	0.000113
$C_{D(\text{wave})}$	0.00238	0.00507	0.001665
$C_{D(i)}$	0.00437	0.00000	0.000000

To minimize the wave drag, area ruling was utilized. A wave drag program developed by Boeing was used for the drag analysis. By reducing the size of the fuselage near the mid section, the wave drag was reduced. The cross sectional area distribution for the entire aircraft is shown in Figure 3-8. The final drag breakdown is shown in Figure 3-9. The total drag coefficient for Mach 3.0 is 0.01415 (83,485 lb).

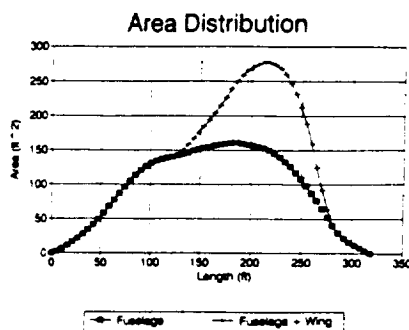


Figure 3.8 Aircraft Cross Sectional Area Distribution

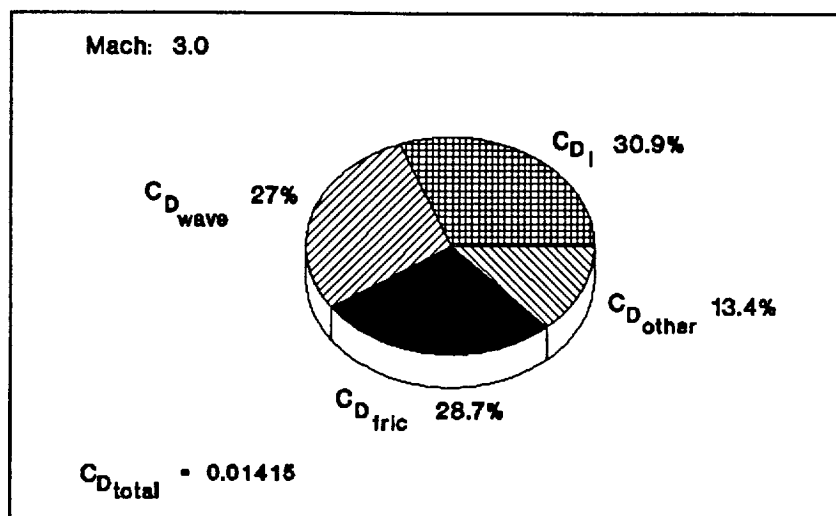


Figure 3.9 Final Drag Breakdown (Supersonic Cruise Condition)

For the subsonic case, the drag breakdown is shown in Table 3-4. The total subsonic drag coefficient is 0.03232 (62,106 lb). The induced drag accounted for 74 percent of the total drag, while friction and other drag sources accounted for 12.8 and 13 percent of the drag, respectively.

Table 3-4

Total Aircraft Drag Breakdown
(Subsonic)

	M = 0.7 Wing	H = 30,000 ft Fuselage	AR = 1,69 Tail
$C_{D(total)}$	0.02615	0.00205	0.000175
$C_{D(f)}$	0.00195	0.00205	0.000175
$C_{D(i)}$	0.02420	0.00000	0.000000

4.0 PROPULSION SYSTEMS

4.1 Engine Candidates

In order for the Supercruiser to achieve a cruise Mach number of 3.0, the range specified in RFP 1A, and be environmental acceptable, its engines must provide a considerable amount of thrust with a low specific fuel consumption and low noise emission. In this section, the following engines will be reviewed as potential SST propulsion systems: turbojet, turbofan, and variable-cycle engines.

4.1.1 Turbojet

The price for supersonic speed is the afterburner, which on the turbojet is economically unfavorable at subsonic speeds. However, at Mach numbers above 2.5, the afterburning turbojet becomes more efficient due to the pressure rise linked with diffusion in the inlet. This will raise the nozzle pressure ratio to a higher value.

Some of the characteristics of the turbojet is listed below:

1. Thrust increases with combustion temperature / decreases with forward speed
2. At high forward speeds, the margin of energy available is small
3. Has relatively high thrust specific fuel consumption at low altitudes and air speeds
4. Small frontal area results in good ground clearance
5. Light specific weight (weight per pound of thrust produced)

4.1.2 Turbofan

The turbofan engine has better propulsive efficiency compared to the turbojet engine. The propulsive efficiency is improved by reducing non-dimensional thrust. The main concept for the turbofan is using the energy available to provide a greater mass flow rate at a lower velocity and therefore, as mentioned above, to improve propulsive efficiency.

There are three important parameters introduced by the turbofan. These are (1) the bypass ratio of fan mass flow to main jet mass, (2) the fan pressure ratio, and (3) the energy extraction fraction. The high values of static thrust ratio at low bypass ratios show the usefulness of the turbofan engine for takeoff, which is one of its main advantages.

Some of the characteristics of the turbofan are listed below:

1. Weight greater than that of the turbojet
2. Ground clearance is not as good as the turbojet
3. Low Thrust specific fuel consumption and specific weight
4. Low noise levels. No noise suppressor is required

4.1.3 Future Potential Engine Designs

Research has indicated that there are three different engine concepts which seem very promising for future utilization. These three variable cycle engine concepts (VC) are a result of research done by General Electric (GE) and Pratt and Whitney (P & W).

Some of the characteristics of the VC engine are listed below:

1. High available thrust
2. Good subsonic and supersonic SFC
3. Low noise levels
4. Large frontal area

There is no engine concept that exists at this point which will adequately satisfy all HSCT propulsion system requirements. There is a tradeoff between noise-level and range. Therefore, further research and development is needed to meet FAR Part 36, stage 3, noise limits and accomplish the desired range.

4.2 Engine Inlet System

4.2.1 The Inlet

A mixed compression inlet was chosen for the Supercruiser. The external compression is to be achieved by double wedge variable geometry ramp splitter system (see Figure 4-1a). The splitter (entire double wedge ramp system) translates horizontally to insure that shock wave impinges on the cow lip. The total range of travel for the splitter system from Mach 1.5 to Mach 3.0 would be 8.5 ft (the total distanced traveled can be reduced if structural, mechanical, or weight problems arise; however this would reduce total pressure recovery). The internal compression system consists of three variable geometry ramps with the subsonic transition occurring at the normal shock located at the intersection of the ramp shocks (see Figure 4-1b). Following the transition to

subsonic flow the air would be further compressed in the diverging duct until it reached the compressor face.

The maximum mass flow rate of a rubber engine sized by compressor diameter to meet the demands of an HSCT aircraft was calculated. The mass flow rate was determined to be 607.15 lb/sec per engine. Thus the total mass flow rate for the two engine pod inlet system is 1215 lb/sec. The total cross-sectional capture area for the two engine inlet was determined to be 95.82 ft². From this value, the inlet height and width were determined to be 6 ft and 15.97 ft, respectively. The total inlet length was calculated to be 55.37 ft (again if structural or weight problems occur this length could be reduced by decreasing the subsonic compression length; however again this would be accompanied by a decrease in total pressure recovery). For this design, the total pressure recovery (P_{o_c}/P_{o_w}) was determined to be 0.757 at Mach 3.0.

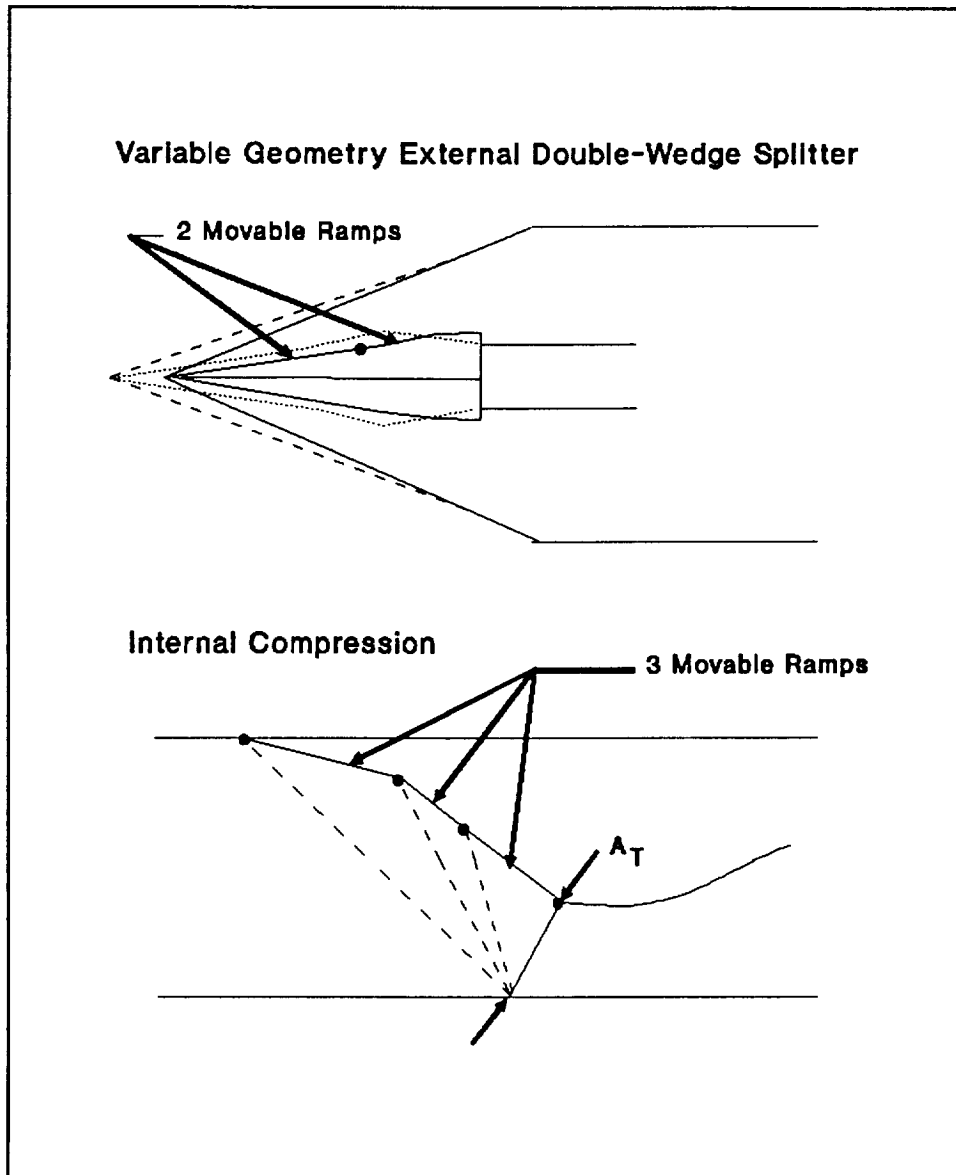


FIGURE 4-1. Inlet System: (a) External Compression System
(b) Internal Compression System

4.2.5 Future Design Considerations

The inlet design is an important part of the conceptual design of the aircraft. It was for this reason that the time was taken to develop an inlet design for a rubber engine since no current engine has been selected for the aircraft. It is also for this reason that the initial design of the inlet only encompasses the most basic elements of the design process. Once the actual engine is selected, the following improvements can be made to the inlet design: The optimum ramp angles can be determined for all the stages of acceleration to cruise. One of the variable geometry ramps can be replaced by an isentropic compression ramp. The engine can be angled to reduce the expansion corner experienced at the point of transition from external to internal compression. The effects on the pressure recovery of the boundary layer removal system can be determined. Finally, the subsonic diffuser length can be optimized. These additional refinements would be expected to increase the pressure recovery between 0.80 and 0.87 at Mach 3.0.

5.0 STRUCTURAL ANALYSIS

5.1 Structures (General)

In supersonic aircraft structures, over 75% of the primary structural weight is for buckling, crippling, and stiffness. To reduce this weight, sandwich construction panel methods are utilized instead of the conventional skin-stringer stiffening design. Sandwich construction offers higher strength-to-weight ratios, better stability and load carrying capacity, increased fatigue life, and higher sonic fatigue resistance. Sandwich construction structures have the potential of reducing the structural weight by 12% to 25%.

Advanced composite materials are utilized to further reduce the weight of the aircraft. With composite materials, the best material properties are utilized for maximum material load carrying efficiency. The fibers are oriented in the direction of the load to make the best use of its high strength and stiffness properties. Materials are tailored to the structure to minimize weight.

5.2 Material Selection

In selecting materials to construct an HSCT, many important factors must be taken into account in order to select the "best" material. The best material depends on its particular application. Factors that must be considered are yield and ultimate strength, stiffness, density, temperature limit, fatigue, crack resistance, fracture toughness, corrosion, creep, cost, and producibility.

Since the Supercruiser will operate above Mach 2.0, the skin of the aircraft will experience temperatures ranging from -50 °F to 600 °F. Hence, the chosen material must be able to withstand extreme temperature variances. Furthermore, the chosen materials must also have high strength-to-weight, and stiffness-to-weight ratios in order to keep the aircraft weight as low as possible so that fuel consumption is kept at a minimum. In addition, these materials must be able to maintain their integrity so that the transport will require minimum maintenance and repair through its 15 to 20 year life span.

After comparing various types of materials, it has been determined that composite materials are best suited for the Supercruiser. Composite materials have excellent specific strength and stiffness characteristics. The specific strength and stiffness of composites are about 3 to 5 times greater than aluminum. An all composite aircraft has the potential of reducing its empty weight by 25 to 30 percent in comparison to an all aluminum aircraft. Figures 5-1 and 5-2 are comparisons of specific strengths and stiffnesses for various types of materials. Note that thermal expansion for composites are about 5 to 10 times less than that of titanium. This would greatly reduce the thermal expansion problem that high speed aircraft encounter while in flight.

The Supercruiser will use high temperature, unidirectional fiber polymeric and metal matrix composites. The fiber will be graphite and the matrix materials will be thermoplastic, thermoset, and aluminum. In selecting composite materials, some additional

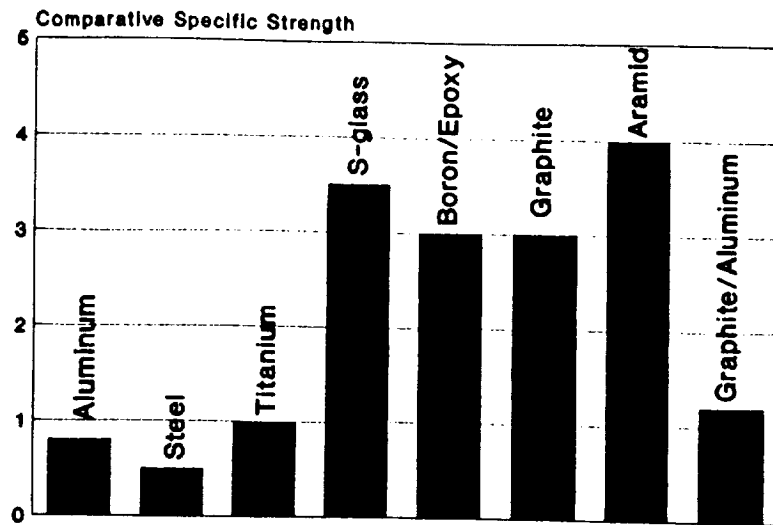


FIGURE 5-1. A Comparison Of Composites And Metals By Specific Strength (Ultimate Tensile Strength/Density)

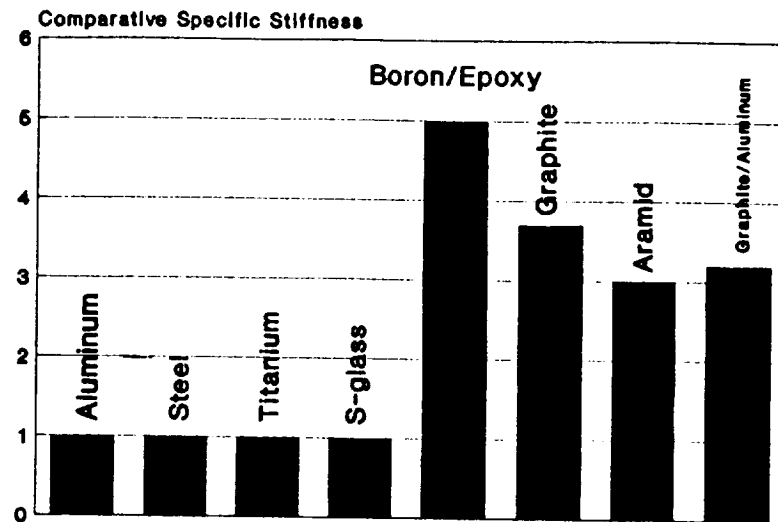


FIGURE 5-2. A Comparison Of Composites And Metals By Specific Stiffness (Modulus/Density)

aspects that must be considered are moisture absorption, impact resistance, thermal stability, and thermal expansion. In comparison to polymeric composites, aluminum metal matrix composites have better thermal stability, better impact resistance, and no moisture absorption problem. However, aluminum metal matrix composites have higher thermal expansion than polymeric composites.

Currently, there are composites that can operate in the temperature regime of the Supercruiser. Graphite/polymide and aluminum metal matrix composites can operate in environments exceeding 600 °F, but they do not have enough thermal stability to meet the required life cycle of the aircraft. In addition to thermal stability, impact resistance is another property that must be improved. More research is required for a better understanding of these materials. For the Supercruiser, the feasibility of using composites will depend on their development in the next 10 to 15 years.

5.3 Thermal Management

When cruising at Mach 3.0, aerodynamic heating is a problem that requires investigation. The skin temperature can reach 600 °F. Therefore, the Supercruiser must be properly insulated in order to maintain a comfortable cabin temperature as well as keeping the fuel below its boiling point. A temperature distribution of the Supercruiser at Mach 3.0 is shown in Figure 5-3.

Criteria for insulation sizing included insulation weight and thickness, and heat flux into the cabin and fuel. A typical cross section of the fuselage and wing is represented in Figures 5-4 and 5-5. The fuselage shell consists of a graphite-polymide/ aluminum honeycomb core panel, a layer of insulation, an air gap, and the cabin lining. The wing shell construction is exactly the same as the fuselage except that the insulating material is attached to the fuel tank instead of the skin panel.

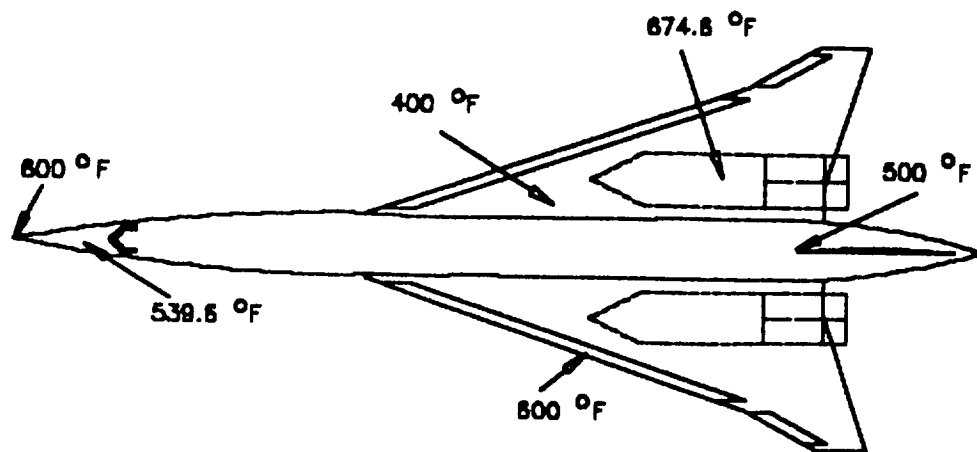


FIGURE 5-3. A Temperature Distribution Of The Supercruiser At Mach 3.0

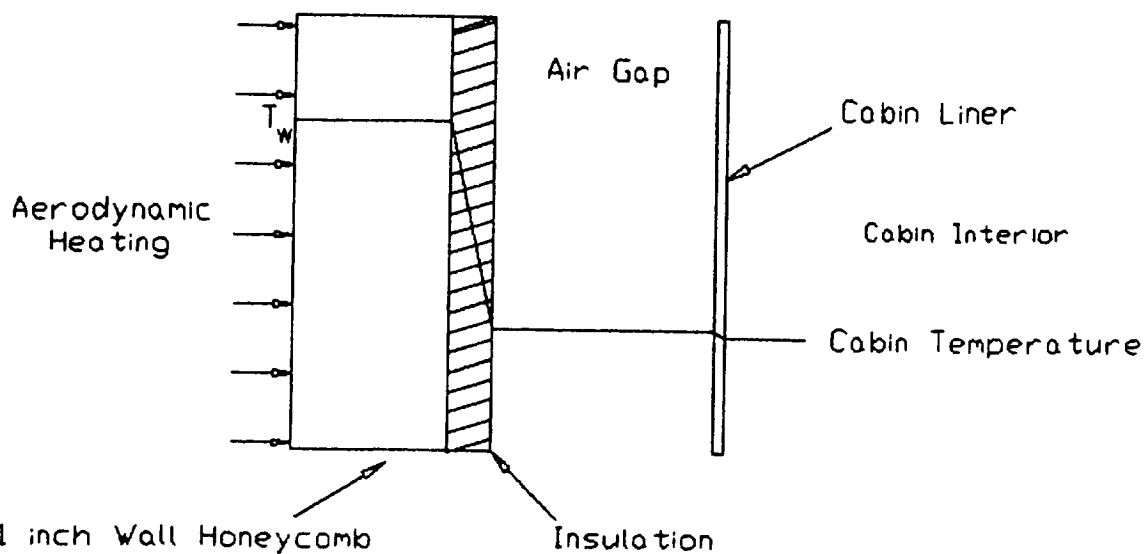


FIGURE 5-4. Fuselage Insulation Design

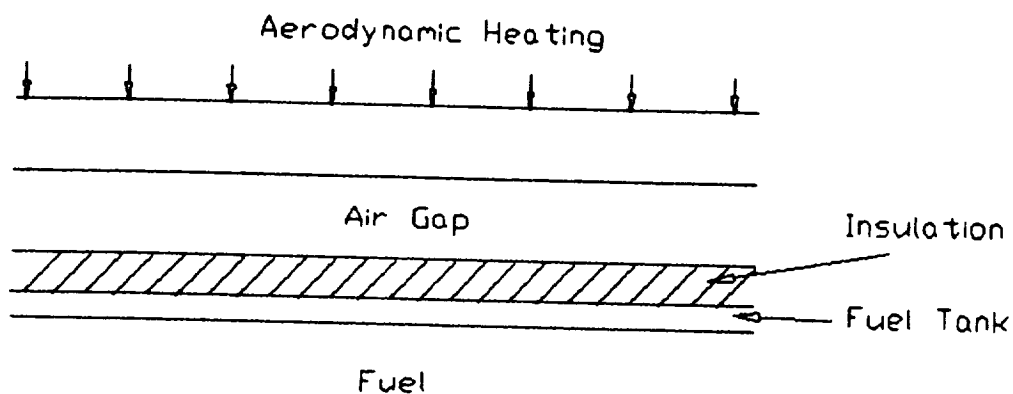


FIGURE 5-5. Wing Insulation Design

The sizing constraints that were set for the analysis are as follows: the maximum cabin wall heat flux is 30 BTU/hr/ft² to meet the environmental control system; cabin wall and air temperatures are kept at a constant 80 °F and 70 °F, respectively; the maximum allowable fuel temperature is 200 °F; and the maximum insulation thickness is 1 inch. Heat transfer through radiation is assumed negligible and heat flux is one dimensional.

From the above constraints and assumptions, it was determined that the thermal conductivity coefficient K of the insulating material must be less than 0.00139 BTU/hr. Currently there are no insulating materials available that meet this thermal conductivity coefficient value. Information on insulating material with such low thermal conductivity and high temperature application is classified. If such materials do exist, the insulation thickness for the front, mid, and aft sections of the fuselage are 1.0, 0.88, and 0.88 inch, respectively. The insulation for the wing was determined to be 0.37 inch. Active cooling will be required for the engine inlet and nozzle, leading edge, and nose tip.

5.4 Wing Structure

In the wing structure, most of the fibers in the web of the spars and ribs are oriented in the +45 and -45 deg direction to carry the shear load; while most of the fibers in the flange are oriented in the 0 deg direction in order to carry the bending load. For the skin, the laminate consists mostly of [90,-45,+45] plies to carry the bending and torsional load.

For the Supercruiser, the face sheets of the sandwich skin panel consist of 18 plies of graphite polyimide with the fibers oriented in the $[0, -45, +45, 90]$ deg directions. The ply ratio of the laminate are 8-4-4-2 in the $[0, -45, +45, 90]$ deg direction, respectively. A schematic of the laminate is shown in Figure 5-6. The laminate is stacked up symmetrically to prevent tension and twisting coupling. Aluminum is used for the honeycomb core. The cell size ranges from 1/8 to 1/4 inch. Smaller cell sizes are required for bolt connection areas. A cross-section of the skin panel is shown in Figure 5-7. The layout of the spars and ribs are shown in Figure 5-8.

In the sandwich construction, most of the bending load is carried by the skin. The spars and ribs carry a very finite amount of the distributed load. Thus, the spars and the ribs on the wing are very thin. They are primarily designed to carry some of the bending load, as well as, for structural stability purposes.

Graphite Polyimide Laminate	
Ply No.	Ply Direction
1	0°
2	
3	
4	
5	45°
6	
7	-45°
8	
9	90°
10	
11	-45°
12	
13	45°
14	
15	0°
16	
17	
18	

FIGURE 5-6. Graphite Polyimide Laminate Schematic

Wing Sandwich Construction

(Unit - Inch)

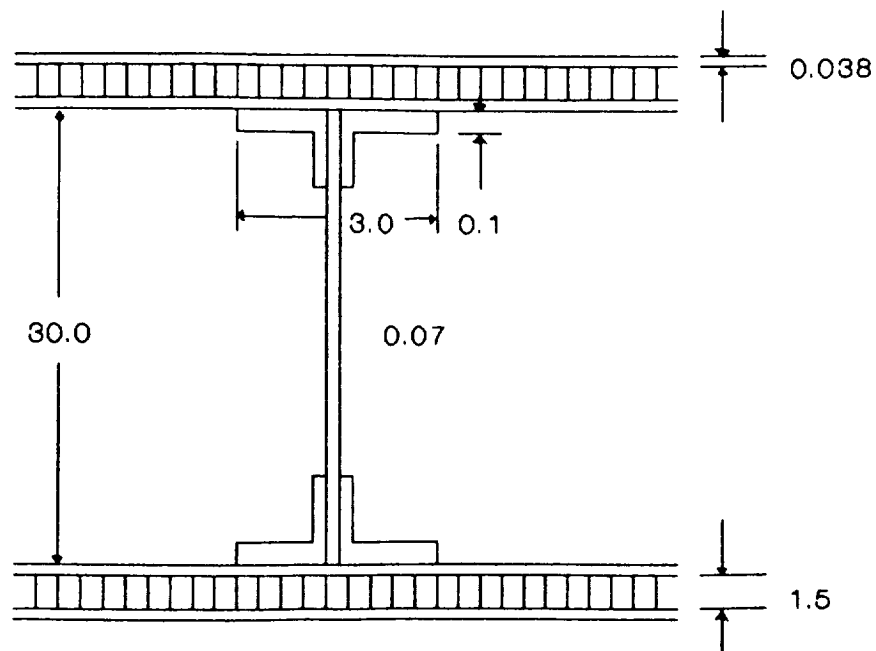


FIGURE 5-7. Cross-Section Of The Skin Panel

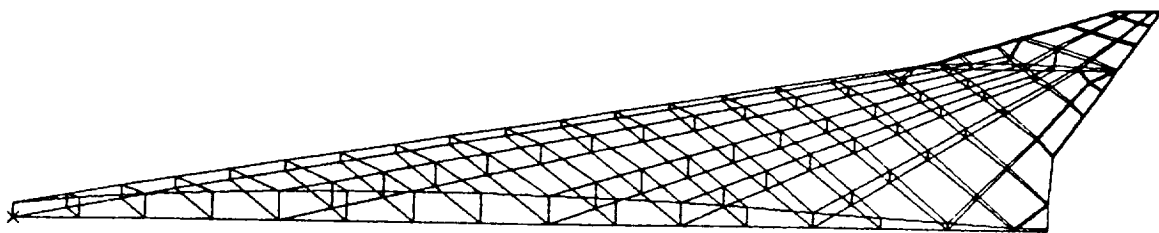


FIGURE 5-8. Spars And Rib Lay-Out Of The Wing Section

A Finite element (FE) analysis was conducted using I-DEAS for structural sizing. The finite element model of the Supercruiser's wing is shown in the figure above. The model represents the skin panel, spars, and ribs. It consists of 208 nodes and 672 elements. In the FE model, the 18 ply laminate was modeled as a 7 ply laminate and the honeycomb core was modeled as an orthotropic laminate. The face sheets and the honeycomb were combined into one element. Quadrilateral and triangular thin shell elements were used to model the wing skin panels, spar, and ribs webs. A beam element was used to model the flange.

The total force on the wing for a 3g lift load is 960,000 lb. For the double delta wing configuration, the first 20 feet of the wing span from the root will carry 50% of the total load while the next 20 feet and the last 20 feet of the span will carry 32% and 17% of the total load, respectively. Material properties for aluminum honeycomb, high strength, and high modulus graphite polyimides are listed in Table 5-1. Since information for material properties at only 450 °F was available, analysis was conducted for a 3g loading at that temperature (see Figure 5-9). After determining the stresses and the deflections on the wing structure, it was determined that stiffness was more important than strength. Therefore, high modulus graphite polyimide was chosen for the aircraft.

For the wing, the thickness of the web and flange of the ribs and spars are 0.1 and 3.0 inch, respectively. A honeycomb core thickness of 1.5 inches is needed in order to provide enough

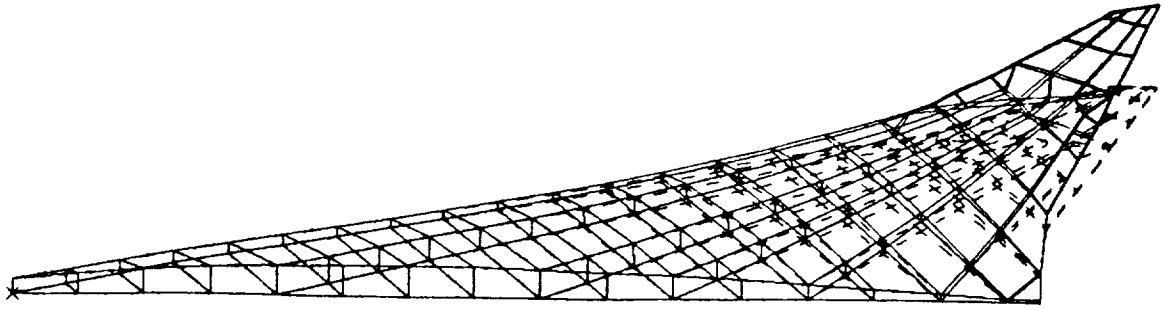


FIGURE 5-9. Wing Deflection (3g Loading)

stiffness for bending, buckling, and fluttering. For this design, the maximum tip deflection for 3g loading is 6.42 feet. Furthermore, Tsai-Wu failure criteria was used to check for laminate failure. All the laminates were well below the maximum failure index, and the strain energy was located at the center of the wing. For structural optimization, thicker spars will be required in this region; however, the thickness of the spars and ribs everywhere else can be reduced to minimize the weight.

5.5 Fuselage Structure

The fuselage of the Supercruiser, as shown in Figure 3-7, utilizes the sandwich construction concept described in the Wing Structure section. The stiff skin panel greatly reduces the size of the ring frame and longerons. As in the case of the wing, the bending load was carried by the skin panel.

The fuselage structural elements are primarily designed based on the loading conditions defined below.

5.4.1 Loading Conditions

Dynamic heating: At the nose tip of the Supercruiser, it is expected that the skin temperature at a cruise condition of Mach 3.0 could reach 600 °F. Representative temperatures and temperature gradients at certain fuselage stations are obtained from experimental data of the NASA supersonic aircraft model 969-512B (Ref. NASA CR-2667).

Fuselage concentrated loads: The calculated static load of the nose landing gear acting at fuselage station 99 ft from the nose tip is 82,751 lb. Reaction loads at the wing root due to a load factor of $n=3$ are the primary loads considered in the design of the wing box.

Pressurization: Pressurization of the fuselage was analyzed using the pressure gradient between the inner and the outer wall of the fuselage. Assuming standard atmospheric conditions, the pressure difference was calculated to be 2022 lb/ft².

5.4.2 Fuselage Structural Elements

The fuselage structure is divided into three sections; forward-, mid-, and aft-section. In general, the three sections have similar semi-monocoque structures. However, for each section, specific design criteria drew special attention. Dynamic heating,

complex wing box structure, and tail fuselage connection presented ultimate conditions in designing structures for the forward-, mid- and aft-section, respectively.

Fuselage Forward-Section Structure: The forward-section structure covered the fuselage section from zero to 99 ft. The sandwich shell construction is the primary structural design concept. The supporting frames are joined using mechanical fastening and bonding. The nose tip skin should be made of Ti-alloy whose temperature limit is high enough to withstand the dynamic heating problems incurred at Mach 3.0.

Fuselage Mid-Section Structure: The primary structure of this section is the wing box construction. A design concept of the wing box is based on the typical design of most modern transport aircrafts in which main frames of the fuselage are bolted to the main spars of the wing box. Both spar moment and shear connections are spliced into the fuselage forward and aft bulkheads. The bulkheads and wing spars are rigidly connected together as one integral unit.

This concept is chosen primarily because of the following factors:

1. It has been widely used and highly reliable.
2. The low wing has relatively high shear and moment reactions at the fuselage and wing intersection when encountering a load factor of $n=3$. Since the bulkheads and the wing spars are an integral unit, cracking due to high shear and moment reactions could be avoided.

3. The wing structure (main spars) could be constructed as a continuous unit. This will ease the fabrication process of composite wing structure.

Fuselage Aft-Section Structure: The main construction concern of this section is the mechanism that supports and rotates the vertical tail. The two main spars of the vertical tail structure are connected to the aft fuselage bulkheads by means of a system of gears driven by a hydraulic system. Design concept of the gear system depends on the size and power of the hydraulic system available.

5.6 Tail Structure

Sandwich construction is also applied to the tail structure. In order to provide stiffness and prevent fluttering, the required thickness of the sandwich panel is approximately 1.0 inch. Two spars and three ribs are used to help support the skin. The tail leading edge could reach temperatures near 479 °F. Therefore, it is suggested that Ti-alloy be used in the leading edge section.

5.7 Landing Gear

The Supercruiser will employ a tricycle landing gear configuration. The location of the gear with respect to the CG location indicates that the overturn angle is 66 deg, which satisfies the requirement outlined by FAA regulations. Calculation of the overturn angle yielded the value of 16 deg, thus guaranteeing that the tail section would not touch the ground at takeoff.

Both the nose and main gear use oleo shock absorbers which have the highest energy absorbing efficiency of all absorbers presently available. It was determined that the main gears' shock absorbers and tire deflections could absorb an amount of energy up to 6.36×10^5 lb-ft.

The nose gear is operated by a hydraulic system which retracts the landing gear system forward and mechanically releases with free fall in emergency conditions. The size of the tires were selected to be 47x18x18 inches with a maximum tire pressure of 175 psi. The twin-wheel nose gear could withstand a maximum static load of 86,000 lb.

The main gear is also hydraulically operated to retract backwards into the wheel-wells located in the inlet housing. Tire sizes were selected to be 52x20.5x23 inches with a maximum tire pressure of 195 psi. The two six-wheel bogie main gear could carry a maximum static load of 732,000 lb. A braking system is installed in the main gear and should be able to withstand a dynamic braking load of 53,000 lb and absorb up to 1.8×10^8 lb-ft of braking energy.

6.0 PERFORMANCE

6.1 Takeoff Distance

The takeoff distance for the Supercruiser was calculated. In this analysis, a factor of safety of 1.5 was applied to the stall velocity. In addition, the acceleration was assumed to be constant (the average acceleration was used), and no high lift devices were incorporated for this situation. Therefore, the calculated takeoff distance was determined to be 9,287 ft. This distance is within the 10,000 ft limit set by the RFP. Because the takeoff distance value was close to that dictated in the RFP, flaps had to be incorporated in order to ensure the takeoff requirement. The addition of leading-edge flaps significantly improved the takeoff performance of the Supercruiser. With the flaps deployed, the takeoff distance was reduced to 7,429 ft.

6.2 Range and Endurance

6.2.1 Range

The range of the Supercruiser was calculated. For a supersonic cruise flight profile (ie. the entire block time at Mach 3.0), the range was calculated to be 3183 nmi. On the other hand, for a subsonic cruise flight profile (ie. the entire block time at Mach 0.8), the range was determined to be 1,421 nmi. It is clear that both the subsonic and supersonic cruise ranges of the Supercruiser do not meet the required range proposed by the RFP. Although, considering the current technology, it is unlikely that the range

will meet the RFP requirement, however, it can be increased. Figure 6.1 shows that range increases in direct proportion to the value of $C_L^{1/2}/C_D$. Thus by optimising the break point on the double delta (ie. improving the $C_L^{1/2}/C_D$ ratio) an increase in range can be achieved. In addition, range analysis of the current configuration has shown that the optimum range would be achieved by operating the aircraft at a Mach number of 2.6 instead of 3.0. Since the range is a primary driver, the reduction of the Mach number to 2.6 would probably be a viable method of increasing the range even though it adversely affects the economics involved due to the higher trip time. In addition to decreasing the Mach number, the analysis has shown that, decreasing the altitude in conjunction with the Mach number could offer an improved range (see Figure 6.2).

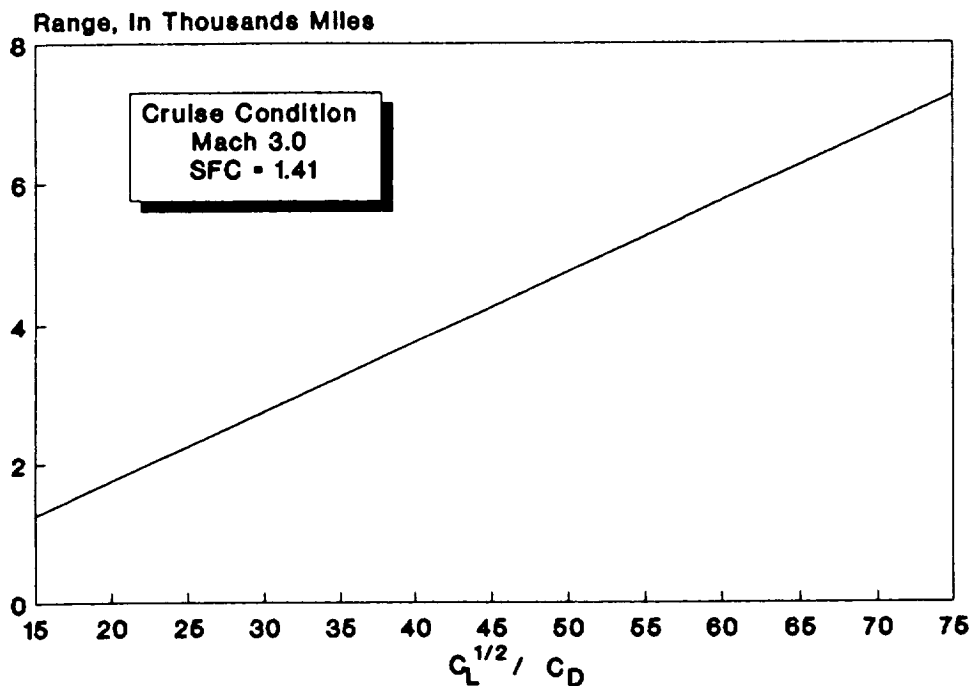


FIGURE 6-1. Range As Function Of $C_L^{1/2}/C_D$

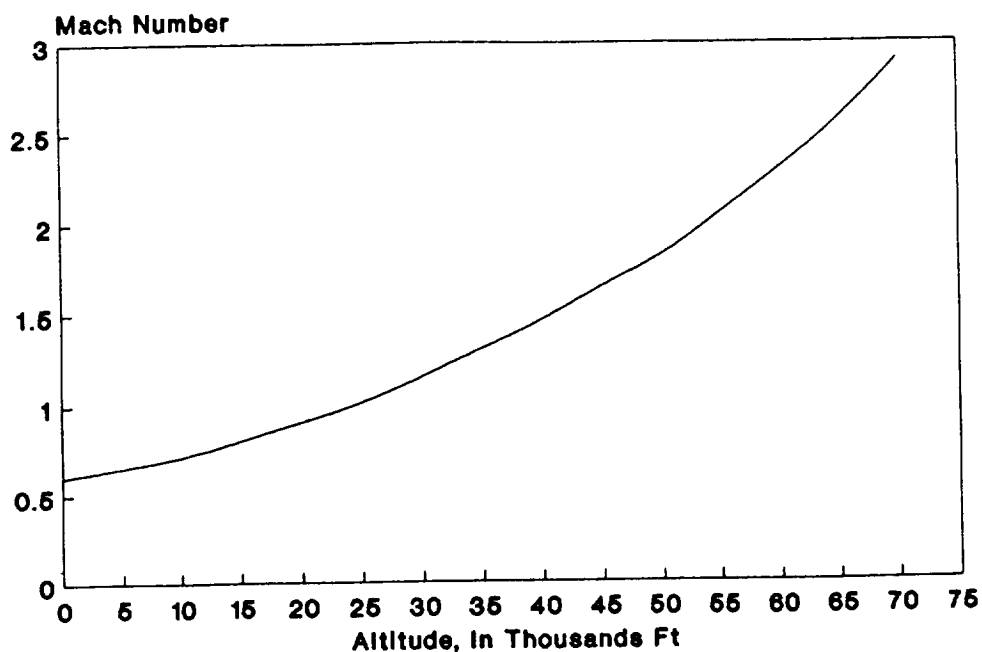


FIGURE 6-2. Optimum Mach As A Function Of Altitude

Looking to the future for technological advances in engine specific fuel consumption is another option. If the SFC of the Supercruiser's engines could be reduced to .513 (per engine), the range would increase to 5500 nmi. To reach a range of 6000 nmi, the SFC would have to be reduced to .470 (per engine), and to reach the 6500 nmi point, the SFC (per engine) would have to be reduced to .434.

Thus, as described in the above paragraph, the possibility of increasing the range of the aircraft does exist. This possibility is attainable with both the current and future technology. To capitalize on these possibilities the following steps should be taken:

1. Optimize the break point location on the double delta wing to improve the $C_L^{1/2}/C_D$ ratio
2. Modify the cruise Mach number and altitude to those determined to be optimum by the range analysis
3. Improve the specific fuel consumption of the engines

6.2.2 Endurance

For the range calculations, a General Electric Mach 2.5 design engine was incorporated. This engine was hypothetically designed by General Electric for future high speed civil aircrafts. Since this engine was designed for a maximum speed of Mach 2.5, it was necessary to size the engine for a cruise Mach number of 3.0. Figure 6-3 shows a plot of endurance as a function of specific fuel consumption. Note, the endurance for the supersonic cruise condition at Mach 3.0 and an altitude of 60,000 ft is only 1.64 hours. This value appears to be rather low. Thus the process of the sizing and resulting endurance calculations are taken to be extremely conservative.

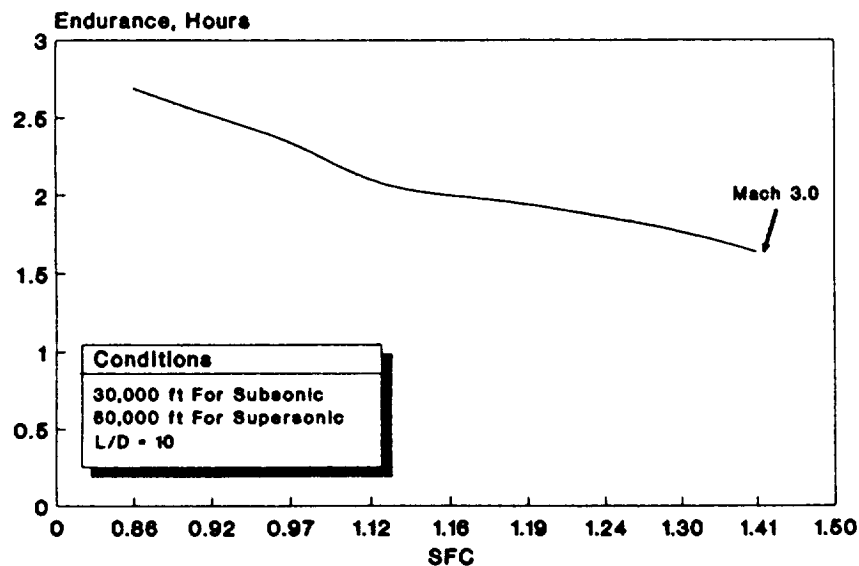


FIGURE 6-3. Endurance As A Function Of SFC

6.3 Landing Performance

The landing distance for the Supercruiser was calculated. The approach distance and transition distance was calculated to be 1395 ft, while the landing distance was determined to be 6052 ft. The landing distance was calculated for the Supercruiser with spoilers only. Utilizing 15% thrust reversal, the landing distance was determined be 5805 ft.

Figure 6-4 shows the effect of $(C_L)_{\max}$ on landing distance. Presently, no design changes are needed since the landing distance is well within the allowable limit of 10,000 ft.

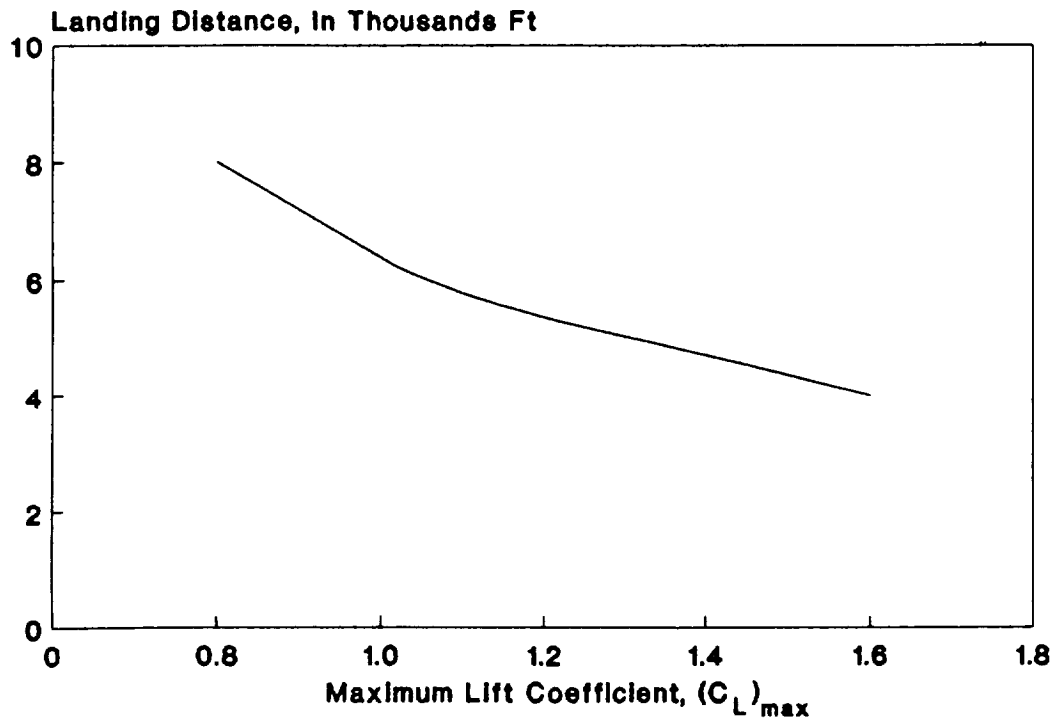


FIGURE 6-4. Effect Of $(C_L)_{\max}$ On Landing Distance

6.4 Takeoff and Landing Visibility

Good visibility from the flight deck is essential for the following reasons:

- (1) During takeoff and landing operations, the pilots must have a good field of vision of the immediate surroundings.
- (2) During enroute operations, the pilots must be able to sufficiently observe conflicting traffic.

Because the Supercruiser's nose tip doesn't rotate downward, the visibility pattern is limited to a specific field of vision. Furthermore, because the flight deck windows are curved so as to offer low drag, they may lead to image distortions. In an attempt to correct the Supercruiser's takeoff and landing visibility problem, Apogee Aeronautics will devise a camera system strategically located in the lower forward section of the nose cone. The camera system will be flush with the fuselage's surface and will be exposed only during takeoff and landing sequences. Moreover, this system will project the images it scans and reproduce them on a imaging screen located on the pilot's control station. The system will be redundant thus meeting the safety standards incurred by FAA regulations.

6.5 Rate Of Climb

Rate of climb of the Supercruiser varied as it traverses through the subsonic, transonic, and supersonic flight regimes. Utilizing the basic energy relationship, the climb rate for each flight regime was determined. Using the Concord

as a baseline, the following climb rates were used:

Immediately after takeoff (up to altitude of 3,000 ft), the climb rate was calculated to be 17 ft/sec

Subsonic climb rate (6 to 23,000 ft), 89 ft/sec

Transonic climb rate should be lower than that of subsonic regime or it could be negligible because in this regime of high drag the pilot would use the excess power to accelerate quickly out of the transonic regime rather than climbing the aircraft.

6.6 Rate Of Descent

The distance required to accomplish normal descent of a typical supersonic aircraft from end-of-cruise altitudes to the point at which the initial approach was commenced would be at a range of 200 nmi. Typical rate of descent for the Supercruiser was calculated to be 4000 ft/min in the supersonic range. Once it reached the subsonic cruise, aircraft maneuvering was no longer restricted to the same extent as that of the supersonic speed, the rate of descent could be adjusted in order to adapt to the present flight conditions.

7.0 STABILITY AND CONTROL ANALYSIS

7.1 Subsonic

It was determined earlier that the Supercruiser was stable during supersonic cruise conditions. Now it is necessary to determine whether it is stable subsonically. Stability of the aircraft is most important subsonically because of the possibility of crashing during takeoff and landing. Furthermore, subsonic stability analysis was necessary because the aircraft was not designed with a horizontal tail; it was necessary to determine if the aircraft would be longitudinally stable without the use of an elevator. In the following analysis, a cruise altitude of 30,000 ft and a Mach number of 0.7 were used.

The longitudinal analysis revealed that the aircraft is stable longitudinally. From the characteristic equation, it was observed that the phugoid mode was split up into two real roots and the short period had two complex roots. The results are as follows:

Longitudinal Stability Analysis

PHUGOID MODE

Time constants	8.29 and 1.09
Flying quality	Level 3

SHORT PERIOD

Damping ratio	0.20
Undamped natural frequency	3.67
Flying quality	Level 2

All of the roots were located in the left half of the s-plane and there was adequate damping for the short period; therefore, the aircraft was stable longitudinally. The aircraft oscillates for about two seconds and then stabilizes quickly. The pitch angle response, on the other hand, is very well damped and does not oscillate, thus reaching a steady value. The longitudinal stability analysis confirms that the aircraft is stable longitudinally; therefore, it can operate without a horizontal tail so long as other pitch and elevation controls are provided.

Analyzing the lateral response of the aircraft, it was observed that the aircraft did not have adequate controls. The aircraft had two real roots on the left half of the s-plane and one pair of imaginary roots on the right half of the plane. The imaginary roots on the right half plane made the aircraft unstable laterally. The results are as follows:

Lateral Stability Analysis

DUTCH ROLL MODE

Damping ratio	-0.4
Undamped Natural Frequency	2.89

SPIRAL MODE

Time constant	27.427
Flying quality	Level 2

ROLL MODE

Time constant	0.32
Flying quality	Level 1

The dutch roll mode is unstable and cannot be classified for this current aircraft configuration.

It is recommended that the longitudinal mode flying qualities be improved via a stability augmentation system (SAS). The damping of the system needs to be improved to achieve Level 1 flying qualities. For the lateral stability, the tail should be sized to stabilize the dutch roll mode.

7.2 Cruise Stability

The Supercruiser's supersonic cruise stability is suprisingly well-behaved. Cruise stability is achieved without the use of ailerons or a horizontal tail. Instead, cruise stability is achieved by the management of the aircraft's center-of-gravity (CG). The aircraft's CG management gives it natural stability without the use of a stability augmentation system (SAS). Although complete stability was not achieved in all realms of lateral motion, management of the CG allowed for a less complex stability enhancement system.

Since flying qualities at supersonic cruise are well behaved, Level 1 flying qualities were achieved with the short period mode. A 42 sec period was achieved with a time-to-half amplitude of 9.360 seconds. A divergent damping ratio of -0.124 was found for the phugoid mode which resulted in a 2 min period, thus achieving an

unstable phugoid mode. Level 1 flying qualities were achieved in the spiral mode. A time constant of 122.8 sec was achieved. A Level 3 roll mode was also achieved, with a time constant of 3.33 sec. An unstable, divergent dutch roll resulted. A divergent damping ratio of $-.656$ and a period of 37.56 sec was the result. The unstable phugoid and dutch roll modes were found to have very long periods. This will allow the pilot adequate time to adjust the flight controls or for the stability augmentation system to compensate for the divergent reactions to perturbations.

7.3 Transonic Stability

Transonic stability is always a matter of concern for aircrafts that have to travel through this flight regime. Most supersonic aircrafts spend the least amount of time in this regime. The flight requirements for the Supercruiser is a transonic descent to the airport. Therefore, it would be beneficial to investigate transonic flight stability. Transonic flight stability is difficult to examine because of the complexities and uncertainties of transonic flight itself. Instead, Mach numbers nearing the transonic flight regime (Mach 1.4 at 35,000 ft.) will be examined, and some conclusions will be extrapolated from the resulting data.

Flying qualities at Mach 1.4 degrade as compared with the supersonic cruise element of the aircraft. However, phugoid and short period modes improve. Level 1 flying qualities are achieved for the phugoid mode. A damping ratio of $.049$ with a period of 314 sec is achieved. A very damped short period is achieved with the

short period mode. Because of the very damped short period, the flying qualities cannot be determined. Values for the damping ratio are so close to the real axis that it can be generally assumed that the short period mode is completely damped. Level 1 flying qualities is achieved only with a w_m of .4 for the Dutch Roll mode. Spiral mode is still Level 1, but the time constant degrades to 49.722 sec. Roll mode is maintained at Level 3, however, the time constant degrades to 1.876 sec. A SAS system is highly recommended as the Supercruiser's speed approaches the transonic flight regime.

8.0 FUSELAGE INTERIOR LAYOUT

8.1 Passenger Seating Arrangements

The main driver for the passenger seating arrangement was that the Supercruiser was to be capable of accommodating for 300 passengers including baggage, eight flight attendants, and a flight crew of two. With these parameters in mind, the maximum diameter of the fuselage was calculated to be 17.1 ft. The diameter of the fuselage at specific points along its length was dictated by area ruling and a wave-drag computer simulation program. This was necessary in order to reduce supersonic drag.

Due to marketability demands, the seating arrangement was designed by considering a tri-class arrangement as shown in Figure 8-1. The three class seating arrangement is as follows: 7-, 36-, 57-percent for first, business, and economy classes, respectively. The first class section is positioned in the forward zone of the fuselage, the business class section is positioned in the mid-zone, and the economy class section is in the aft portion of the fuselage. A 20 inch minimum aisle width and 84 inch aisle height accommodates passenger space requirements. Represented in Figure 8-2, seat widths are 47 inch double-seat assembly for first class, 40 inch double-seat assembly for business class, and 39 inch double-seat assembly and 55.5 inch triple-seat assembly for economy class. The first, business, and economy classes have a four-across, six-across, and seven-across seating arrangement, respectively. The comfort levels for the passengers are

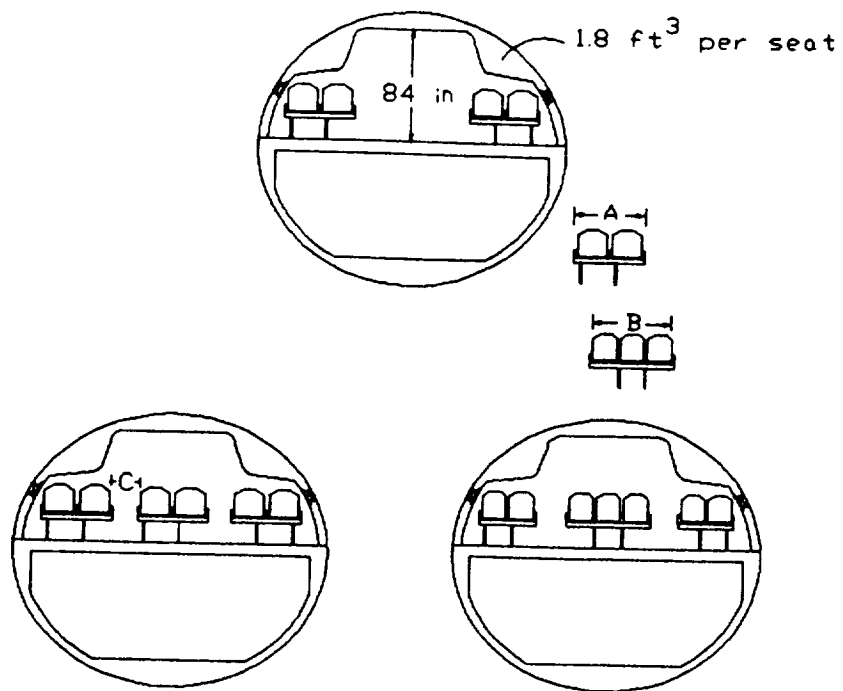


FIGURE 8-1. Tri-Class Seating Arrangement

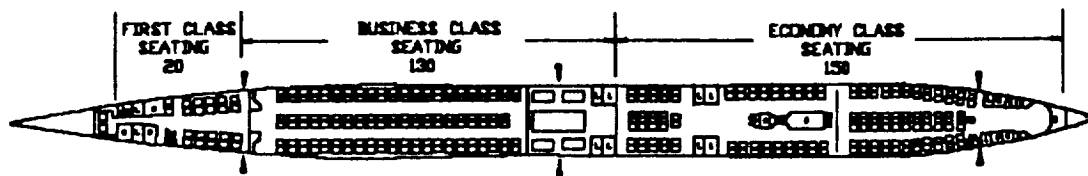


FIGURE 8-2. Cross-Section Of The Fuselage

implemented at a level comparable with the standards of current subsonic carriers.

8.2 Capacity and Payload Accommodatons

The Supercruiser's cargo/baggage holds are designed in order to accommodate for the passengers baggage and secondary items such as freight and mail. The overhead stowage bins, which are located along both sides of the entire cabin, are capable of holding 1.8 cubic feet per passenger. While lower cargo bays, located underneath the cabin floor, are proportionally sized for multi-shelf containers. The lower cargo bays, or belly holds, are situated so that the weight of the cargo doesn't adversely affect the center of gravity location. Thus, the belly capacity per passenger seat is set around 8 cubic ft and the baggage weight per passenger is averaged around 45 lb.

In order not to incur additional costs, the Supercruiser will be utilizing standard containers and pallets currently being used by other airline carriers. One benefit of the pallets and containers is the fact that they greatly reduce the loading time of baggage and cargo. Furthermore, a roller system designed into the belly holds will facilitate loading and unloading. Note that while the aircraft is in flight, the pallets and containers are secured by tie-downs, thus preventing the cargo from sliding and thereby changing the CG location.

8.3 Interior Facilities

The interior facilities provides contemporary service for 300 passengers based on a maximum flight duration of 4 hours. Each class (first, business, and economy) has its own galley, lavatories, closets, and cabin attendant stations. The cabin attendants are adjacent to each exit door.

Interior facilities such as service areas and lavatories are positioned with the maximum interior flexibility in mind. Table 8-1 lists the number of facilities located within each class section, while Figure 8-1 shows where these facilities can be found within the cabin. Each class section has its own service area and other interior facilities that are equal to those standards set by long-haul subsonic carriers. Furthermore, flight entertainment is provided by separate view-screens located in each class section and music control units located on each seat. As for the protection of passengers from lethal doses of ozone and radiation, a climatisation system is installed as to deliver maximum climatic comfort comparable to subsonic carriers.

8.4 Doors, Emergency Exits, and Windows

Since all doors, emergency exits, and windows are potential sources for leaks, noise, drag and excess weight, the engineers at Apogee Aernautics designed the above mentioned items so as to maximize passenger comfort and meet those emergency requirments dictated by the FAA. The number and the particular size of doors and emergency exits required in the HSCT type aircraft are

TABLE 8-1

Number Of Facilities Located Within Each Class Section

Section	Attendant	Closet	Galley	Lavatory
First Class	1	1	2 units	2
Business Class	3	2	2 units	5
Economy Class	4	2	3 units	5
Total	8	5	7 units	12

defined in FAR 23 and 25 parts 807-813. The number and type of required exits for the Supercruiser was dependent upon the number of passengers carried.

Since all doors and emergency exits must meet the "unobstructed access" criteria, the designers used Type I, II, and III access doors to fulfill this requirement. As shown in Figure 8-3 and given in Table 8-2, there are a total of 6 access doors: two passenger Type I doors, two emergency Type II doors, and two emergency Type III doors. The dimensions are given in Table 8-2. Service access doors are located mainly on the starboard side of the aircraft, however, there are some also located on the port

side.

Each emergency exit and the two passenger doors are equipped

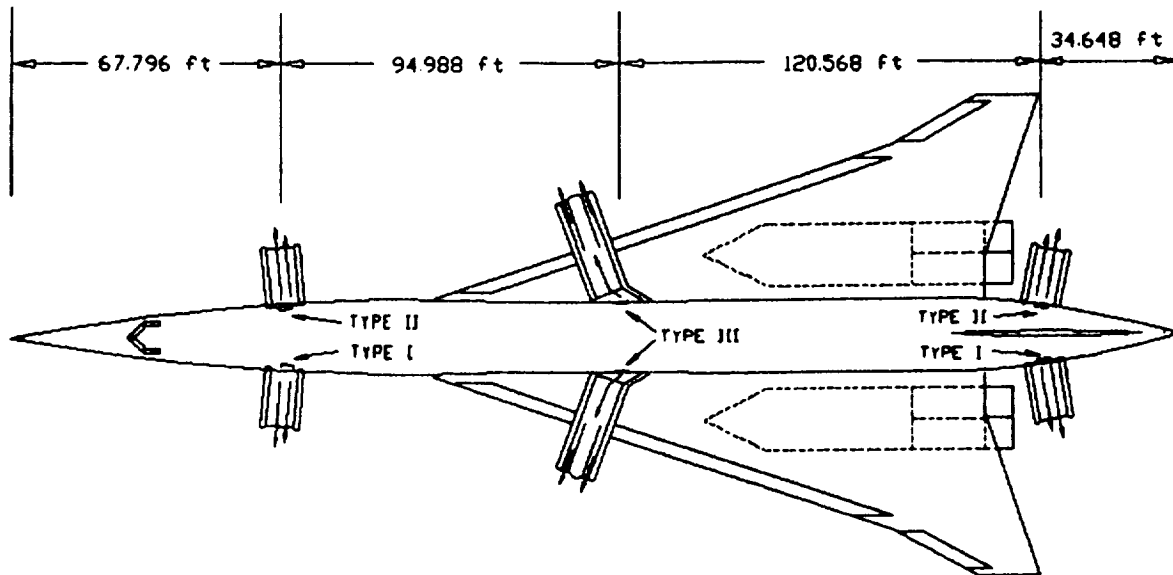


FIGURE 8-3. Location Of Access Doors/Emergency Slides

TABLE 8-2

Number And Dimensions Of Access Doors

ACCESS DOOR		TYPE	DIMENSIONS
Passenger Doors	(2)	I	6.0 X 3.0 ft
Emergency Exits	(2)	II	3.7 X 1.7 ft
	(2)	III	3.0 X 1.5 ft

with a Emergency Escape Chute Deployment System. This system is composed of evacuation slides that are deployed in case of an emergency. The following are the characteristics of such a system:

1. Inflatable slides automatically deploy upon opening each exit
2. Inflation by stored gas
3. Escape system disarmed when door opened from outside of airplane
4. Slides usable in all landing gear conditions

Note that standard life rafts would be stowed in overhead stowage bins located near each emergency exit and passenger door.

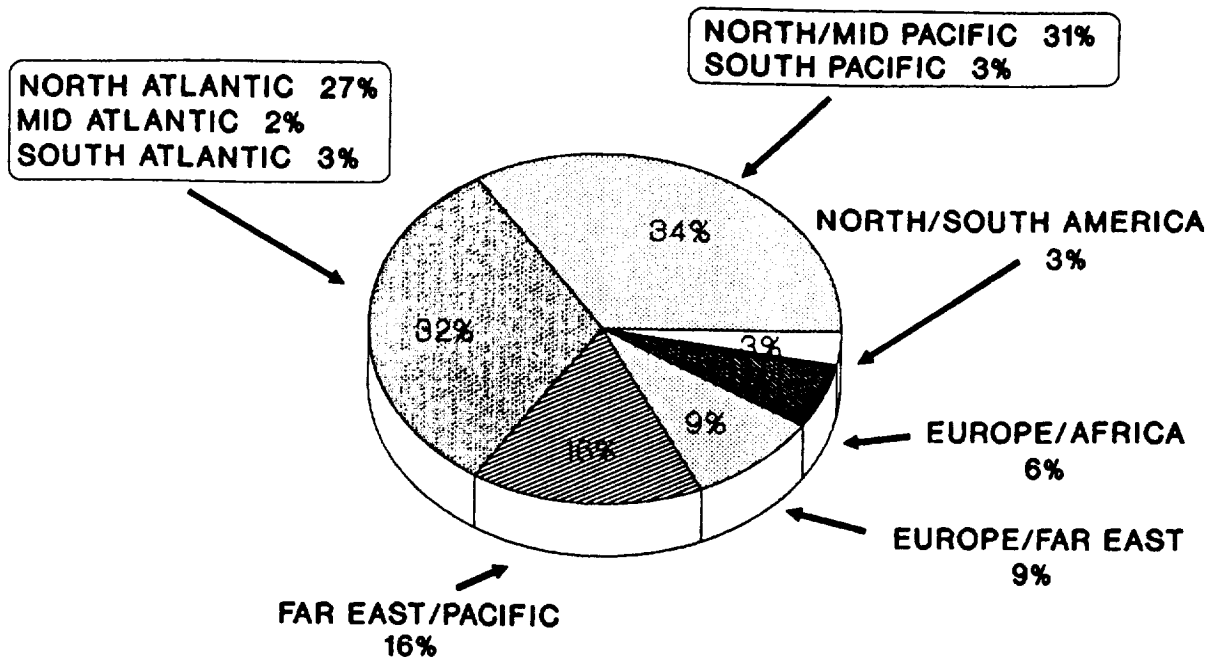
The passenger windows on the Supercruiser are circular and are spaced according to the fuselage's frames and not necessarily spaced according to passenger seat location. This particular shape of the window is utilized in order to avoid unnecessary stress concentrations and large pressure differentials that may be encountered while flying supersonically. The windows are located so that there is no discomfort to the average passenger when viewing through them.

9.0 MARKETABILITY

9.1 Potential Markets

In order to produce a viable HSCT, the market demand had to be sufficient enough as to sustain a fleet of approximately 500 aircrafts. A preliminary analysis determined that the Supercruiser could acquire a significant portion of the growing long-range, Atlantic and Pacific Rim markets. Present statistical data projects that the worldwide demand for long-range air travel will almost double by the year 2000, with a growth potential of 53% in the Pacific Basin and 27% in the North Atlantic region. Figure 9-1 shows the international traffic distribution based on the year 2000 with a traffic distribution of 200,000 passengers per day. This figure shows that the greatest market demand is located in both the Atlantic Rim and Pacific Rim regions.

The Supercruiser's potential as a viable long-range carrier is dependent not only on the market demand but also on its performance characteristics such as speed, design range, and total amount of passengers carried. For this airplane configuration, the speed is fixed at Mach 3.0 and the range was determined to be below 4000 nmi. Even though the range falls short of the expected 5500 nmi, the effectiveness of the Supercruiser to capture a proportional amount of revenue passenger miles (RPM) depends upon which market it is operating within. The revenue potential for the Pacific and Atlantic Rim markets are as follows:



TOTAL FOR YEAR 2000: 200,000 PASSENGERS PER DAY

FIGURE 9-1. International Traffic Distribution

first class projected 6% of total revenue, business 45%, and economy 49%. Therefore, by concentrating on the revenue potential, the Supercruiser can be a viable addition to the current long-range carriers operating in these markets.

9.2 Airport Compatibility

Operations from conventional airports requires that the Supercruiser must meet anticipated weight and field-length constraints, as well as operating in conjunction with subsonic carriers during approach to avoid system degradation. Since the Supercruiser weighs less than 800,000 lb and takes off within 12,000 ft, it can be accommodated by selected high-demand airports such as Los Angeles Airport (LAX) and Tokyo Airport (NRT). The high speed of travel and the high altitude of the Supercruiser doesn't require special equipment on part of the Air Traffic

Control (ATC) services. Since the Supercruiser will be outfitted with enhanced avionic systems, it will easily integrate into the ATC environment.

Because the Supercruiser is considerably larger than subsonic carriers such as the 747-400 (length of 231.8 ft), some modifications to the runway fillets may be necessary in order to maintain an acceptable runway-edge safety margin while maneuvering on the ground from runway-to-taxiway and taxiway-to-taxiway intersections with the cockpit over the centerline. Figure 9-2a represents the potential fillet requirements necessary in order to safely operate the Supercruiser at high-demand airports. The camera system mentioned in the takeoff and landing visibility section can be utilized for ground roll maneuvers.

As shown in Figure 9-2b, gate parking in front of a terminal can be achieved with the Supercruiser positioned at an angle. Because of the Supercruiser's length and door sill height, minor adjustments might have to be made in order to connect the passenger entrance embilical to the passenger doors.

Supercruiser servicing operations will be tasked such as to minimize 'turn-around' time as much as possible. As shown in Figure 9-3, a large amount of servicing vehicles must be able to have simultaneous access to the aircraft while it is parked at the gate. The required trucks and other servicing vehicles for the Supercruiser are listed in Table 9-1. Typical services such as load and unloading of passengers and cargo, refuel, and recoil are pertinent tasks that must be performed in a minimal amount of time.

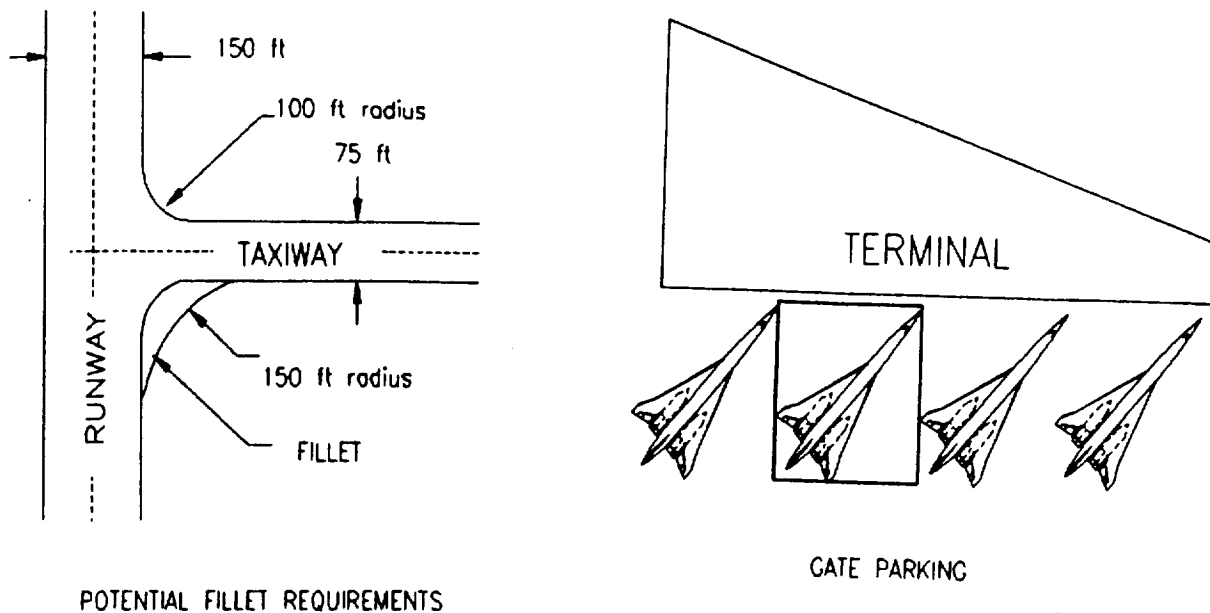


FIGURE 9-2. (a) Runway Fillet Requirements (b) Gate Parking

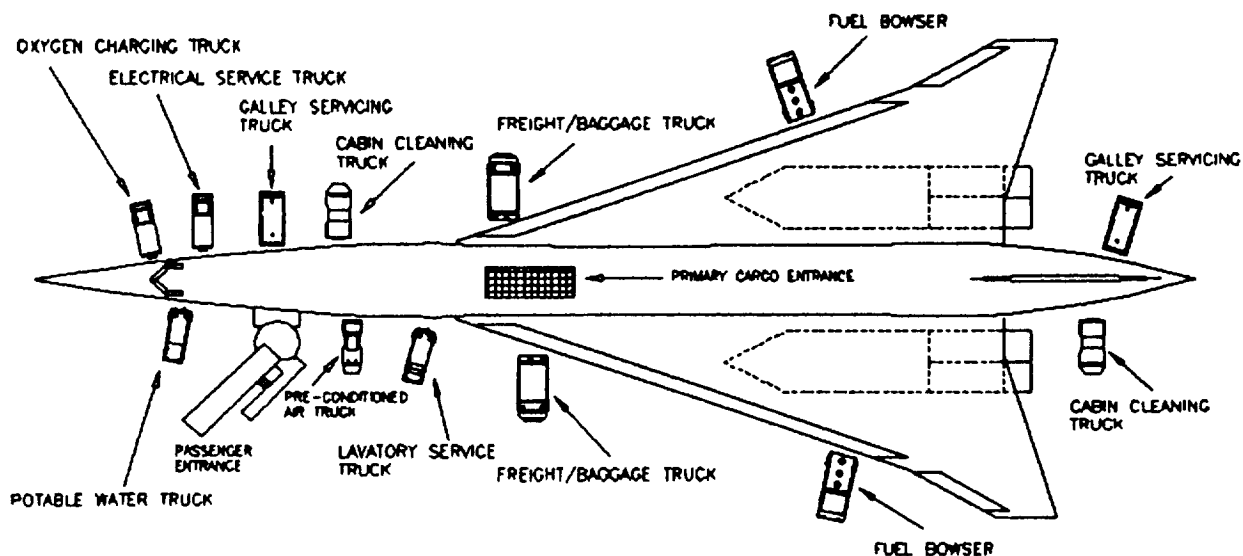


FIGURE 9-3. Servicing Vehicle Layout

TABLE 9-1

Required Trucks And Other Servicing Vehicles

SERVICE VEHICLE	# OF UNIT(s)
Cabin Cleaning Truck	2
Electrical Service Truck	1
Freight/Baggage Truck	2
Fuel Bowser	2
Galley Servicing Truck	2
Lavatory Service Truck	1
Oxygen Charging Truck	1
Potable Water Truck	1
Pre-Conditioned Air Truck	1

9.3 Cost Analysis

For the Supercruiser to become marketable and meet the demands of future air travel, it must be cost effective within its life cycle. Utilizing a cost analysis computer simulation program, the Supercruiser was determined to be unprofitable with its current range of 3183 nmi. This shortfall is mainly dependent on current technological advances. However, a cost analysis for the Supercruiser was generated assuming that technology by the time of its introduction, around the year 2015, would increase its range from 3183 nmi to 5500 nmi. This presumption is not inconceivable since a parameter such as the weight can be dramatically reduced thus increasing the range and thereby reducing the total cost of the aircraft.

Table 9-2 shows the cost analysis that was performed on the Supercruiser. The table lists the input data that was used in order to determine the three primary costs: Research, Development,

Test and Evaluation cost (RDTE), manufacturing and acquisition cost (MACQ), and operating cost (OPS). Table 9-3 lists the operating cost per block hour and the total operating cost per block time for the Supercruiser. The beforementioned primary costs are summed up to equal the life cycle cost (LCC) of the Supercruiser's program. The LCC being considered over a 16 year period. Note that a estimated cost for a prototype program consisting of 2 airplanes cost roughly 423 million 1992 United States Dollars (USD).

TABLE 9-2

Cost Analysis Breakdown

CALCULATIONS IN 1992 DOLLARS

INPUT DATA:

TOTAL WEIGHT OF SUPERCRUISER (WT) = 760000 lbs
 MAXIMUM VELOCITY (VM) = 1983.685 kts
 RANGE (DI) = 5500 nm
 NUMBER OF PASSENGERS (NX) = 300
 NUMBER OF ENGINES (NE) = 4
 NUMBER OF AIRPLANES PRODUCED (NM) = 500
 NUMBER OF AIRPLANES PRODUCED FOR RDTE (NR) = 5
 NUMBER OF AIRPLANES FOR PROTOTYPE PROGRAM (NT) = 2

SUPERCRUISER COST DATA:

RESEARCH, DEVELOPMENT, TEST AND EVALUATION COST (CS) = 2.563693E+10 USD
 MANUFACTURING AND ACQUISITION COST (B4) = 6.689164E+10 USD
 OPERATING COST (Z3) = 1.118146E+12 USD

ESTIMATED UNIT PRICE PER AIRPLANE (AEP) = 1.850572E+08 USD
 ESTIMATED MARKET PRICE PER AIRPLANE (AMP) = 1.28118E+08 USD
 ESTIMATED COST OF PROTOTYPE PROGRAM (PROT) = 4.236957E+08 USD

LCC = CS + B4 + Z3

LIFE CYCLE COST OF THIS AIRPLANE PROGRAM (LCC) = 1.210675E+12 USD

TABLE 9-3
Operating Cost Per Block Hour

<u>DIRECT OPERATING COST</u>	1992_USD
CREW	265.60
FUEL & OIL	14,291.75
INSURANCE	472.23
TOTAL FLYING OPERATION COST	15,029.58
TOTAL MAINTENANCE	3,175.03
AIRFRAME DEPRECIATION	2383.88
ENGINE DEPRECIATION	133.88
AVIONICS SYSTEMS DEPRECIATION	152.04
AIRPLANE SPARE PARTS DEPRECIATION	387.88
ENGINE SPARE PARTS DEPRECIATION	114.75
TOTAL DEPRECIATION	3,172.43
LANDING FEES	376.20
NAVIGATION FEES	2.47
REGISTRY TAXES	203.06
TOTAL FEES	581.73
TOTAL FINANCE COST	1,652.80
TOTAL DIRECT OPERATING COST	23,611.57
<u>TOTAL INDIRECT OPERATING COST</u>	11,805.79
TOTAL OPERATING COST PER BLOCK HOUR	35,417.36
TOTAL OPERATING COST PER BLOCK TIME (4.04 hrs)	143,192.39

In order to accurately surmise the cost evaluation of the Supercruiser, it was compared against three potential competing carriers: the 747-400 by The Boeing Co., the MD-12 by Douglas Aircraft Co., and the A340-300 by Airbus Industrie. These three

carriers represent the primary competition that the Supercruiser will face in the 21st century. Figure 9-4 shows the cost comparison with the competitive carriers. Note that the Supercruiser does cost more initially, however, as more units are sold the cost becomes considerably less. Also, a unit production of 1200

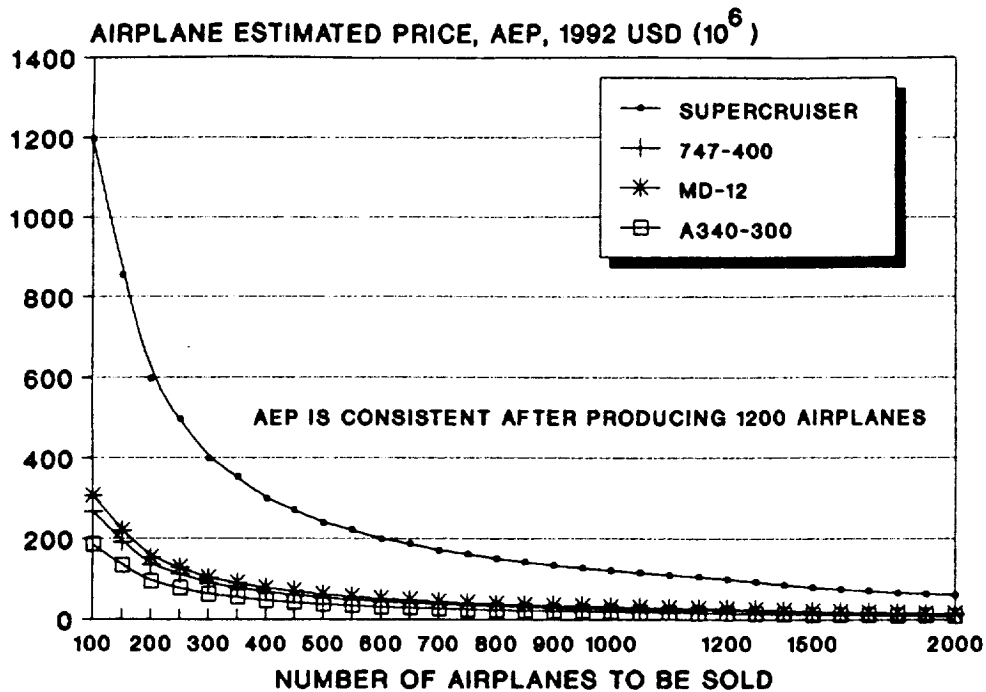


FIGURE 9-4. Cost Comparison With Competitive Carriers

aircraft is suggested in order to be profitable in its LCC. It was determined that the operating cost of the Supercruiser and its LCC is three times less than the competing carriers.

In a competing market such as the airlines industry, one of the primary drivers for market capture is the airfares charged to passengers. In order for the Supercruiser to be competitive, its airfares must be comparable to those of the competing subsonic

carriers. For ranges greater than 5000 nmi, coach fares are set between \$600 and \$800 1992 USD. These fares were determined from current airlines such as United, Northwest, and American. To be competitive, the Supercruiser must charge a coach fare rate between \$650 and \$950 1992 USD. This coach fare is based on a range greater than 5500 nmi, 80% of available seats filled, and a profit range between 10% and 62%. The 80% of available seats filled is exceptable in current subsonic carriers. In addition, the profit range mentioned above is considered acceptable for continuing operations. Utilizing the same methods to determine the primary costs, it was determined that the Supercruiser meets the above criteria for the coach fare charged to passengers. Therefore, if a range of 5000 nmi was achieved, the Supercruiser will be a profitable carrier and a competitive opponent of the subsonic carriers.

10.0 Maintenance and Reliability (M & R)

10.1 Engine M & R

10.1.1 Maintenance

The maintenance of the engines is one of the important aspects in selecting the engine. The following considerations are taken in order to make engines more maintainable.

1. The engine will be chosen to be operated with thermally stable jet fuel.
2. The engines will be separated and installed in individual nacelles.
3. Engine build-up units will be interchangeable on wing position.
4. Easy and fast accessibility of engines and accessories should be provided.
5. An engine change should be possible during one shift time. Specialized ground equipment should be kept to a minimum.

All the above specifications are taken in consideration when selecting an engine.

10.1.2 Reliability

The reliability of the engines will be evaluated by the engine manufacturer. Since the engines considered for the Supercruiser do not exist at this point, there is not much evaluation that can be done regarding reliability. As a matter of fact, the engines by GE and P & W are not expected to be certified until around 2010.

10.2 Materials M & R

Composite structures will always have some form of flaws and defects. Because of the multiphase nature of the material and the processes used in its manufacturing, a substantially higher number of defects may exist in a composite component than that would occur in metallic components.

Two common types of damage for composite structures are delamination and impact damage. Delamination can be due to environmental effects or by fatigue. When the damage is detected, the damage section is removed. A new piece is put in using specified adhesive to bond the two pieces together. The patch is vacuum-bagged under pressure, and heat is applied to the materials. The patch is then sanded and painted. If the damage is too big, the entire composite laminate will be replaced.

In the low temperature regime, composites have proven to be quite durable and reliable. Boron and graphite epoxy tails of F-14 and F-15 manufactured 15 to 20 years ago are still in service. In high temperature environments, composites have not proven to be as good as they are in low temperature environments. Thermal stability and impact resistance need to be improved in order for composites to be used for high speed aircraft.

11.0 ENVIRONMENTAL IMPACT

11.1 Sonic Boom

The environmental disturbance of the sonic boom is well known by those individuals who live near certain military facilities. As a result of the annoyance of this disturbance, a major request of the RFP called for supersonic flight over land without the disturbance of the sonic boom felt on the ground. The above request is for the time being impossible. Many tests have been conducted which aimed at determining the maximum levels of over pressure (measure of sonic boom intensity) which could be produced by supersonic aircraft which would be acceptable to the public and the environment. The results of such studies have varied. Depending on the author of the study, the range of acceptable over pressures is from as low as no increase in over pressure to a maximum increase of 0.5 to 1.0 psf. At the present time, the absolute best levels of over pressure that can be achieved are about 1.5 psf. As a result, it is not expected that the HSCT will be allowed to travel over land supersonically in the near future.

11.2 Engine Emissions

NASA contractor report 4233 (September 1989) states that a technically viable HSCT must, under normal operation, have no effect on the existing ozone layer. Effects of engine emissions (No_x) on the ozone layer have yet to be determined and further research is required in order to set standards acceptable to the

and engine-combustion technology as they relate to the reduction of No_x emissions. Studies indicated that the greatest potential for No_x reduction results from the concept of the lean premixed and prevaporized combustion. This concept, however, has the highest technical risk. Technically less of a challenge is the stage-lean combustion which provides less of an No_x reduction. The rich-burn, quick-quench combustion is another possibility, since it has a significant No_x reduction and a lower development risk.

FAA code book title 14, Part 36, subpart D explains that noise limits for the HSCT must fall within parameters set forth in Appendix A, B, and C of said Part 36. This section has a detail and complex description for acceptable testing conditions for aircraft noise levels. It relies to a large extent on the effective perceived noise level (EPNdB) which is described as being the algebraic sum of the maximum tons corrected perceived noise level and the duration correction factor. $\text{EPNL} = \text{PNLTM} + \text{D}$.

Part 34 of FAA code book title 14 discusses exhaust emission requirements for turbine engine powered airplanes. It defines "aircraft gas turbine engines" as being a turboprop, turbofan, or turbojet aircraft engine. Subpart B (engine fuel venting emissions) discuss requirements applicable to aircraft gas turbine engines of classes T3, T8, TSS, and TF equal to or greater than 8,090 pounds rated output manufactured after February 1, 1974. Class TSS aircraft refers to all aircraft gas turbine engines designed to operate at supersonic flight speeds. Section 34.11 of subpart B states that "no fuel venting emissions shall be

discharged into the atmosphere from any new or in-use aircraft gas turbine engines subject to the subpart." The purpose of this statement is to eliminate intentional discharge of fuel drained from fuel nozzle manifolds. It does not apply to normal fuel separate from joints, fittings, and shaft seals. Subpart C (exhaust emissions), section 34.21, (2), states that gaseous exhaust emissions from each new commercial aircraft gas turbine engine of "classes T3, T8, TSS,TF of rated output equal to or greater than 26.7 kilo-newton (6,000 pounds) manufactured on or after January 1, 1984" shall conform to the following formula:

$$SN = 83.6(r_0)^{-0.274} \quad (r_0 \text{ is in kilonewtons}) \text{ not to exceed a maximum of } SN = 50.$$

Subpart G and H of Part 34 discuss test procedures for engine exhaust gaseous emissions and engine smoke emissions. Test procedures shall be conducted at the following percentages of rated output:

MODE	CLASS OF AIRCRAFT		
	TP (*)	TF, T3, T8 (*)	TSS (HSCT) (*)
Taxi/Idle			
Takeoff	100	100	
Climb out	90	85	65
Descent	NA	NA	15
Approach	30	30	34

(*) analytical correction for variations from reference date conditions and minor variations in actual power setting should be specified and/or approved by the

Administrator.

The length of time set for the test procedures is as follows;

MODE	CLASS OF AIRCRAFT		
	TP	TF, T3, T8	TSS (SST)
Taxi/Idle	26 Min.	26 Min.	26 Min.
Takeoff	0.5	0.7	1.2
Climb out	2.5	2.2	2.0
Descent	NA	NA	1.2
Approach	4.5	4.0	2.3

All emission testing must be conducted with engine warm-up, thus having achieved a steady operating temperature. The administrator of the Environmental Protection Agency (EPA) may approve test procedures for any aircraft engine not susceptible to satisfactory testing by the procedures set forth in Part 34.

11.3 Engine Noise

Noise levels were estimated at the FAR Part 36 reference locations for the Phase III Mach 3.2. The noise levels in the table includes the noise reduction effects of the inverted velocity profile (IVP) and a jet noise suppressor, and a treated ejector for the VSCE concept only. The ejector may not be compatible with the VCE concept single expansion ramp nozzle (SERN).

The Part 36 sideline noise estimates have assumed 12-dB and 5-dB suppression for the VSCE, and VCE concepts, respectively. The sideline noise levels for the Mach 3.2 concept exceed the Stage 3 requirements by 9.5 dB. An additional 2- to 3-dB reduction in sideline noise could be achieved with an operational procedure where engine thrust is reduced early in the flight path. However, the takeoff cutback noise levels would increase slightly due to a lower airplane height over the takeoff monitor.

JET NOISE REDUCTION CONCEPTS

CONCEPT	REDUCTION (EPNdB)* (RE:CONICAL NOZZLE)
INVERTED VELOCITY PROFILE	4-6
SUPPRESSOR	6-8
SUPPRESSOR AND EJECTOR	7-15
THERMAL SHIELD	2-4
POROUS CENTERBODY	2-5

* NOISE REDUCTIONS ARE NOT ADDITIVE

ESTIMATED FAR PART 36 NOISE LEVELS (EPNdB)

ESTIMATED FAR PART 36 NOISE LEVELS (EPNdB)

ENGINE	TOGW(LB)	SIDELINE	TAKEOFF(CUTBACK)	APPROACH
STAGE 3 REQUIREMENTS		102.5	105.4	105
P&W VSCE	769,000	112 (-12)	110 (-8)	106 (-6)

NOTE: Above noise estimates do not include shock cell, duct burner, or turbomachinery noise.

() Suppression assumed excluding IVP.

11.3.1 P & W Noise Estimates

P & W predicted FAR 36 sideline noise over a range of available engine thrust for a 600 pounds per second airflow VSCE, and for a VSCE with storable outer stream jet noise suppressor. The suppressor features 12 chutes with 24 tubes at the outer rim, having a base area to jet area ratio of 2.6. A treated ejector with I/II ratio of 1.6 is included with 1.5 inch deep acoustic treatment similar to and sealed from that used in the VCE Tested program.

Use of independently variable fan and core jet areas is a key feature of the VSCE. This allows optimization of the takeoff part power airflow lapse rate of the VSCE enabling "high flowing" of the engine over a range of takeoff power conditions. The engine thereby maintains maximum airflow and achieves thrust variation primarily through changes in jet velocity.

The VSCE with a suppressor nozzle would normally have a fixed duct stream (suppressor) jet area when deployed over the sideline and community noise monitors. For purposes of this sideline noise

study, however, a variable area suppressor was assumed. This will allow optimization of jet noise at the sideline condition. Once the amount of engine scaling/oversizing for sideline noise has been determined (along with the associated suppressor jet area), that suppressor jet area would then be held fixed at that design duct jet area for future studies such as cutback noise. Full two-stream nozzle variability is still available at all other flight conditions with the suppressor in the stowed position. The major noise sources are the jet mixing noise (high and low frequency components) and the duct burner combustion noise. Jet shock noise is not found to be a significant contributor, except at the lowest powers. A noise benefit on the order of 4 dB was estimated by P & W to be available from a 180 degree circumferential Thermal Acoustic Shield. This benefit should apply to both the jet and duct burner sources at the nozzle.

P & W assumed a four-engine HSCT aircraft with a takeoff gross weight of 769,000 pounds. The four variants of the VSCE candidate engine of the study, with 600 pounds per second design airflow size, are jet noise dominated at this takeoff thrust and are projected to exceed the Stage 3 sideline noise limit.

For engines dominated by jet noise at takeoff powers, one means of reducing sideline noise at a given fixed thrust is to oversize the engines (increased airflow, diameter, and thrust) and operate them at a lower relative power (and exhaust velocity) takeoff condition. The noise penalty associated with increased size engine noise - $10 \log (\text{airflow size})$ - is more than offset by

engine noise - $10 \log (\text{airflow size})$ - is more than offset by operation at a lower percent of full power with attendant reduced jet velocity - jet noise of order - $60 \log (\text{velocity})$. The larger engines, however, are heavier and do not operate at optimal power in the cruise regime, thus having increased fuel burn and either an aircraft takeoff gross weight (at constant range) or range penalty (at constant gross weight).

The basic noise predictions for this study were made for an engine having a 600 pounds per second design inlet airflow (reference) size. The engine can be easily resized using the relationship that noise scales as:

$$\text{Change In SPI} = 10 \log(\text{design airflow}/600 \text{ pps}) \quad [\text{dB}]$$

Similarly, thrust of the 600 pounds per second engine would scale directly as:

$$\text{Thrust} = \text{Ref. thrust} * (\text{design airflow}/600 \text{ pps}) \quad [\text{dB}]$$

12.0 FUTURE DESIGN RECOMMENDATIONS

Technology changes in leaps and bounds. The future poses increased possibility for the impossible to become possible. Limitations become viable and economical alternatives. The current configuration of the Supercruiser includes an inherent lack of yaw control devices. Currently, the all-moving rudder is the only known yaw control device on the Supercruiser. A consideration for the future is the use of the engines to provide yaw control. Engines on either side of the aircraft can be powered up and powered down to create aircraft yaw. This yaw control system can either be controlled manually by the pilot by adjusting engine output power or by a control computer system that is incorporated into the flight control system. This system would be very attractive as the aircraft takes off and lands. At the attitude the Supercruiser operates, the rudder is blanked by the aircraft's fuselage caused by its high angle of attack. The only possible fault about this system is that this could increase engine maintenance hours and engine life, and it could increase fuel consumption.

Another alternative is the use of speed brakes. Speed brakes would decrease landing distance and approach speed. Alternatively, this would increase the angle-of-attack of the aircraft to make up for the loss of lift. Also, the higher angle-of-attack would place more burden on the propulsion system in order to keep aircraft aloft. As it stands, maximum lift of the Supercruiser occurs at a

15 deg angle-of-attack. High angles-of-attack at landing causes concern for clearance of the aircraft's aft section.

Currently, aircraft engine technology has not progressed far enough where we can meet the range requirement of 6,500 nmi. Furthermore, the engine's fuel consumption is much too high, thus reducing the range of the Supercruiser. In order for the Supercruiser to meet the RFP range of 6500 nmi, a more fuel efficient engine needs to be conceived. To meet the range, a specific fuel consumption of 0.3 is necessary. This aircraft is expected to be introduced in the year 2020, by then it is assumed that an engine fulfilling FAR noise and emissions requirements, as well as the necessary fuel consumption and thrust rating, would have been conceived and introduced into the mass market.

13.0 REFERENCES

- Anderson, Jr., John P., Introduction To Flight 3rd Edition, McGraw-Hill, New York, 1989.
- Boeing Commercial Airplane, New Airplane Development; High Speed Civil Transport Study, NASA CR-4233, September 1989.
- Boeing Commercial Airplane, New Airplane Development; High Speed Civil Transport Study, NASA CR-4234, September 1990.
- Brown, Stuart F., Oblique Wing SST. Popular Science, February 1991, pg. 61-63, 90.
- Domack, Christopher S.; Samuel M. Dollyhigh; Fred L. Beissener Jr.; Karl A. Geiselhart; and Edward E. Swanson, Concept Development of a March 4 High-Speed Civil Transport. NASA Technical Memorandum 4223, 1990.
- Douglas Aircraft Company, New Commercial Programs; Study of High Speed Civil Transports, NASA CR-4235, December 1989.
- Douglas Aircraft Company, New Commercial Programs; Study of High Speed Civil Transports, NASA CR-4236, August 1990.
- Final Report, Boeing Commercial Airplane Company: Oblique Wing Transonic Transport Configuration Development. NASA CR-151928, D6-75793, January 1977.
- Johnson, J.T., Delta Wing SST. Popular Science, February 1991, pg 58-61.
- Jr.; Nelms, Walter P., Application of Oblique-wing Technology - An Overview. AIAA-76-943, September 1976.
- HSCT Concept Development Group, Douglas Aircraft Company; High Speed Civil Transport Studies, NASA CR-4375, May 1991.
- McCormick, Barnes W., Aerodynamics, and Flight Mechanics, John Wiley and Sons, New York, 1979.
- Mclean, F. Edward, Supersonic Cruise Technology. NASA SP-472, 1985.
- Raymer, Daniel P., Aircraft Design: A Conceptual Approach, American Institute of Aeronautics and Astronautics Inc., Washington D.C., 1989.
- Roskam, Dr. Jan, Part 1: Preliminary Sizing of Airplanes, Roskam, Aviation and Engineering Corporation, Kansas, 2nd Printing, Kansas, 1989.

- Roskam, Dr. Jan, Part 2: Configuration Designs and Integration of the, Propulsion System, Roskam, Aviation and Engineering Corporation, Kansas, 2nd Printing, Kansas, 1989.
- Roskam, Dr. Jan, Part 3: Layout Designs of Cockpit, Fuselage, Wing and, Empennage: Cutaways and Inboard Profiles, Roskam, Aviation and Engineering Corporation, Kansas, 2nd Printing, Kansas, 1989.
- Roskam, Dr. Jan, Part 4: Layout Design of Landing Gear and Systems, Roskam, Aviation and Engineering Corporation, Kansas, 2nd Printing, Kansas, 1989.
- Roskam, Dr. Jan, Part 5: Component Weight Estimation, Roskam, Aviation and Engineering Corporation, Kansas, 2nd Printing, Kansas, 1989.
- Roskam, Dr. Jan, Part 6: Preliminary Calculations of Aerodynamics, Thrust and Power Characteristics, Roskam, Aviation and Engineering Corporation, Kansas, 2nd Printing, Kansas, 1989.
- Roskam, Dr. Jan, Part 7: Determination of Stability, Control, and Performance Characteristics: Far and Military Requirements, Roskam, Aviation and Engineering Corporation, Kansas, 2nd Printing, Kansas, 1989.
- Roskam, Dr. Jan, Part 8: Airplane Cost Estimation: Design, Development, Manufacturing and Operating, Roskam, Aviation and Engineering Corporation, Kansas, 2nd Printing, Kansas, 1989.
- Shevell, Rrichard S., Fundamentals of Flight, Prentice Hall, New Jersey, 1989.
- Schartz, R.T. and Rosato, D.V., Composite Engineering Laminates.
- Sweetman, Bill; Michael J. Gething; Doug Richardson; Spick Mike; and Gunston, Bill, The Great Book of Modern Airplanes. Portland House, New York, 1987.
- Turner, M.J. and Grande, D.L., Study Of Advanced Composite Structural Design Concepts For An Arrow Wing Supersonic Configuration, NACA CR-2825, April 1978.
- United States Federal Government, Code of Federal Regulations, Title 14, Aeronautics and Space, Parts 1 to 59, 1991.
- Wood, Richard M., Supersonic Aerodynamics of Delta Wings. NASA Technical Paper 2771, 1988.